THE ASTROPHYSICAL JOURNAL, 285:458–474, 1984 October 15

NGC 7213: A KEY TO THE NATURE OF LINERS?

ALEXEI V. FILIPPENKO AND J. P. HALPERN
Palomar Observatory, California Institute of Technology
Received 1984 January 6; accepted 1984 April 23

ABSTRACT

New optical spectra show that the nucleus of the S0 galaxy NGC 7213 resembles those of type 1 Seyferts: emission lines such as [Ne V] λ3426, He II λ4686, and broad Hα are visible, and a nonstellar component accounts for a substantial portion of the continuum at blue and ultraviolet wavelengths. On the other hand, many of the emission-line intensity ratios suggest heating due to shocks, since they are similar to those in Heckman's "low ionization nuclear emission-line regions" (Liners). Lines from neutral and singly ionized species are prominent, and high temperatures seem to be implied by the unusually large strength of [O III] λ4363. This investigation demonstrates that the spectral characteristics are much more consistent with photoionization by a nonstellar continuum than with shock heating.

To avoid serious errors in line strengths, the strong stellar component is accurately removed by subtraction of an appropriate template galaxy. Widths of the remaining emission lines range from $\sim$200 to $\sim$2000 km s^{-1} (FWHM), indicating that clouds having different bulk velocities exist in the narrow-line region. Large differences are seen even in lines which arise from the *same species*, such as [O II] $\lambda\lambda$3726, 3729 ($\sim$300 km s^{-1}) and [O II] $\lambda\lambda$7319, 7330 ($\sim$1000 km s^{-1}). Since the latter (auroral) pair is enhanced in gas of high density ($\sim 10^6$ cm^{-3}) while the former (nebular) lines are dominant where densities are low ($\sim 10^3$ cm^{-3}), physically distinct clouds having vastly different densities are present and contribute unequally to the nebular and auroral components of [O II]. This conclusion also applies to the transauroral and nebular lines of [S II], and is supported by a tight correlation between line width and critical density [$v \propto n_e(\mathrm{crit})^{1/5}$] for 16 forbidden lines.

The observed ratio $R \equiv I([\mathrm{O\ III}]\ \lambda\lambda 4959 + 5007)/I([\mathrm{O\ III}]\ \lambda 4363) = 6.65$ cannot be reproduced at *any* reasonable temperature unless $n_e \gtrsim 10^{5.5}$ cm^{-3}. If $T_e \sim 16000$ K (as in hot photoionized gas), then $n_e \sim 10^{6.4}$ cm^{-3}, and values exceeding 10^7 cm^{-3} are likely if the enhancement of auroral over nebular components in clouds of very high density is considered. This is much larger than the value of $\sim$500 cm^{-3} implied by the $I([\mathrm{S\ II}]\ \lambda 6716)/I([\mathrm{S\ II}]\ \lambda 6731)$ intensity ratio, and exceeds the density normally ascribed to the narrow-line regions of Seyfert galaxies (10^3–10^5 cm^{-3}). Given the great range of densities in NGC 7213, models involving photoionization by a nonstellar continuum are able to reproduce the observed spectrum. High temperatures are *not* implied by the [O III] ratio, and a rather low ionization parameter can give rise to strong emission from neutral and singly ionized species. Moreover, the observed relationship between cloud velocity and density, which is consistent with clouds in Keplerian orbits and a nearly radius-independent ionization parameter, can be understood in terms of the two-phase model of quasar emission-line regions developed by Krolik, McKee, and Tarter. The individual clouds must be optically thick to the Lyman continuum so that each of them includes every ionization stage up to a certain level. High velocities and densities are found closer to the nucleus than low values.

These results may be relevant to Liners as a class, since the small value of R which is sometimes observed could be indicative of high densities rather than high temperatures. This would eliminate the major argument in favor of shock heating in Liners, whose observed spectra are adequately explained by photoionization models in most other respects.

Subject headings: galaxies: individual — galaxies: nuclei — galaxies: Seyfert — line profiles — spectrophotometry — radiation mechanisms

I. INTRODUCTION

NGC 7213 is a nearby S0 galaxy associated with an X-ray source (Halpern and Filippenko 1984, hereafter Paper II). Phillips (1979) showed that its nucleus exhibits broad Hα emission characteristic of Seyfert 1 galaxies, but that the Hα luminosity of $\sim 2 \times 10^{41}$ ergs s^{-1} ($H_0 = 50$ km s^{-1} Mpc^{-1}) is low for type 1 Seyferts. He also noted the absence of obvious broad Hβ emission and the prominence of the stellar continuum.

The narrow-line spectrum is of unusually low excitation; [O III] λ5007, [O II] λ3727, and [O I] λ6300 have comparable intensities, and strong [S II] $\lambda\lambda$6716, 6731 and [N II] $\lambda\lambda$6548, 6583 are visible as well. Heckman (1980) identified these properties in a large number of galactic nuclei (including NGC 7213) known as Liners, and such objects received further attention from Stauffer (1982) and Keel (1983*a*, *b*). The spectra of Liners resemble that of NGC 1052, an E3/S0 galaxy in which shock heating (e.g., Dopita 1977; Shull and McKee 1979) was proposed to explain the low-excitation lines (Koski and Osterbrock 1976; Fosbury *et al.* 1978). Consequently, the emission in Liners is generally attributed to shocks (e.g., Baldwin, Phillips, and Terlevich 1981). On the other hand, many Liners are strong X-ray sources (Halpern and Steiner 1983), and their spectra have recently been reproduced equally well with models involving photoionization by a power-law continuum and a low number of ionizing photons per nucleon, or "ionization parameter" (Ferland and Netzer 1983; Halpern

and Steiner 1983). In addition, careful measurements of [O III] λ4363 in NGC 1052 (Keel and Miller 1983; Rose and Tripicco 1984) imply a lower temperature than found in previous investigations, indicating that shocks might not be necessary. Thus, the origin of activity in these galaxies remains unclear.

Features common to both Seyfert galaxies and Liners make NGC 7213 an important object for closer scrutiny. Moreover, Figure 2 in Phillips (1979) indicates that some forbidden lines have different profiles and might provide insight into the physical conditions. In order to shed light on the line excitation mechanism, new X-ray and optical spectra were obtained. X-ray data and the overall continuum from radio through X-ray energies are described in Paper II, whereas a detailed analysis of the optical emission lines is presented here.

Section II describes the observations and gives a brief overview of the spectrum. The stellar component is carefully subtracted in § III, and § IV subsequently discusses the measurement of various emission lines in detail. Important physical parameters are derived in § V. The Seyfert characteristics of NGC 7213 are reviewed in § VI, and its shock features are reconciled with photoionization models. The arguments may apply to classical Liners as well. Section VII explores theoretical models that can help explain the relationships discovered among the emission lines, and major conclusions are summarized in § VIII.

II. THE OPTICAL SPECTRUM

a) *Observations and Reductions*

NGC 7213 was observed on 1982 August 16–18 UT with the Intensified Reticon (Shectman and Hiltner 1976) attached to the Boller & Chivens Cassegrain spectrograph at the Las Campanas 2.5 m du Pont reflector. Two Bausch & Lomb gratings, each having 1200 grooves mm^{-1}, were used in first order to obtain three spectra at $\lesssim 2.5$ Å resolution. The integration times (s) and wavelength ranges were (1800, 1400, 3000) and (λλ3100–4985, 4455–6355, 5675–7570), respectively. A GG420 filter blocked out second-order light in the red spectrum. Sky subtraction was achieved by measuring the object and sky simultaneously through each of the two entrance apertures (2″ × 4″) separated by 27″.4. Outer regions of the galaxy produced very little contamination of the sky aperture.

Wavelength calibration was made possible by recording the spectra of various comparison arcs, and a dispersion of ∼0.15 Å was obtained by fitting a fifth-order polynomial to the centroids of unblended emission lines. Measurements of atmospheric lines showed that zero-point offsets were likewise very small ($\lesssim 0.2$ Å). The Reticon was exposed to a featureless continuum for a long period of time to facilitate the calibration of pixel-to-pixel variations in the detector sensitivity, and a series of integrations made with different intensity levels demonstrated that continuum coincidence losses were negligible.

Calibration of the overall spectral response on the AB_{79} scale of Oke and Gunn (1983) was achieved by comparison with the faint standard stars GD–248 and G158–100 (Filippenko and Greenstein 1984), which are almost featureless. Since they are located near the celestial equator, the long dimension of the entrance aperture was aligned along the atmospheric refraction to minimize relative light losses (Filippenko 1982*a*). The observations of NGC 7213 were made when the air mass was $\lesssim 1.1$, so a single orientation (E-W) was chosen to ensure that nearly identical regions of the galaxy were sampled each night. At all times the seeing was ∼1″, and two of the three nights were photometric. Application of a constant scaling factor to data from the cloudy night produced excellent agreement in continuum shape with the other spectra. The derived absolute flux is uncertain by $\sim \pm 30\%$, however, since the standards were measured through a 2″ × 4″ aperture (as was NGC 7213).

b) *Brief Overview*

The entire optical spectrum of the central 340 × 680 pc^2 of NGC 7213 ($H_0 = 50$ km s^{-1} Mpc^{-1}), obtained by adding together the three separate spectra, is presented in Figure 1. Data points in overlapping sections were combined in proportion to their statistical weights. A Gaussian with 4.4 Å full width at half-maximum (FWHM) was used to smooth the displayed spectrum, so an unresolved emission line should appear as a spike with thickness comparable to the markers which identify interesting features. Telluric absorption lines were not removed. A Galactic extinction $A_v = 0.05$ mag ($A_v \sim 3.2E_{B-V}$), which is an average of the values from Burstein and Heiles (1982) and from Heiles and Cleary (1979), was adopted to deredden the spectrum. The Whitford (1958) reddening law was used by fitting a quadratic polynomial over the range λλ3000–8000 to points tabulated by Lequeux *et al.* (1979) and Burgess (1958).

Generally speaking, the spectrum resembles that obtained by Phillips (1979). Forbidden lines of neutral, singly ionized, and doubly ionized atoms are prominent, and Hα exhibits both narrow and broad components, the latter significantly redshifted with respect to other features. A corresponding broad Hβ line is weak. The strong underlying continuum is indicative of an old stellar population, but it does not dominate the spectrum to the extent noted previously by Phillips (1979) because of the smaller aperture used here.

An obvious feature is the large range in width of the forbidden lines. [O I] λ6300 is roughly twice as broad as either of the [S II] λλ6716, 6731 lines, for example, and [O III] λ5007 is considerably broader than the blended [O II] λλ3726, 3729 doublet. Even more remarkable is that in some cases *different* lines arising from the *same* ions have disparate widths, as can be seen by comparing [O II] λλ3726, 3729 with [O II] λλ7319, 7330. This clearly indicates that the lines are *not* produced by the same gas; rather, clouds having different bulk velocities must be present, each one contributing to the emission-line spectrum in a manner dictated by local physical conditions.

Lines of Ne^{+4} and He^{+}, as well as the broad Balmer profiles, suggest that a nonstellar continuum similar to that in active galactic nuclei of high luminosity comprises a significant fraction of the flux at blue and ultraviolet wavelengths. Moreover, Paper II shows that a decomposition of the continuum into a "standard" giant elliptical galaxy (Yee and Oke 1978) and a power-law spectrum ($f_\nu \propto \nu^{-\alpha}$) results in a nonstellar component which accounts for at least 50% of the flux at λ3300. The best fit is obtained if the observed continuum of NGC 7213 is initially dereddened by $A_v \sim 0.61$ mag; in this case, the nonstellar component ($\alpha = 1.1$) dominates over the starlight at wavelengths shorter than λ3950 (see Paper II).

III. THE EMISSION LINES

a) *Subtraction of the Stellar Continuum*

The intensities and profiles of emission lines are strongly affected by absorption lines from the bulge stars of NGC 7213, as shown in Figure 1. Since "two-dimensional" data taken

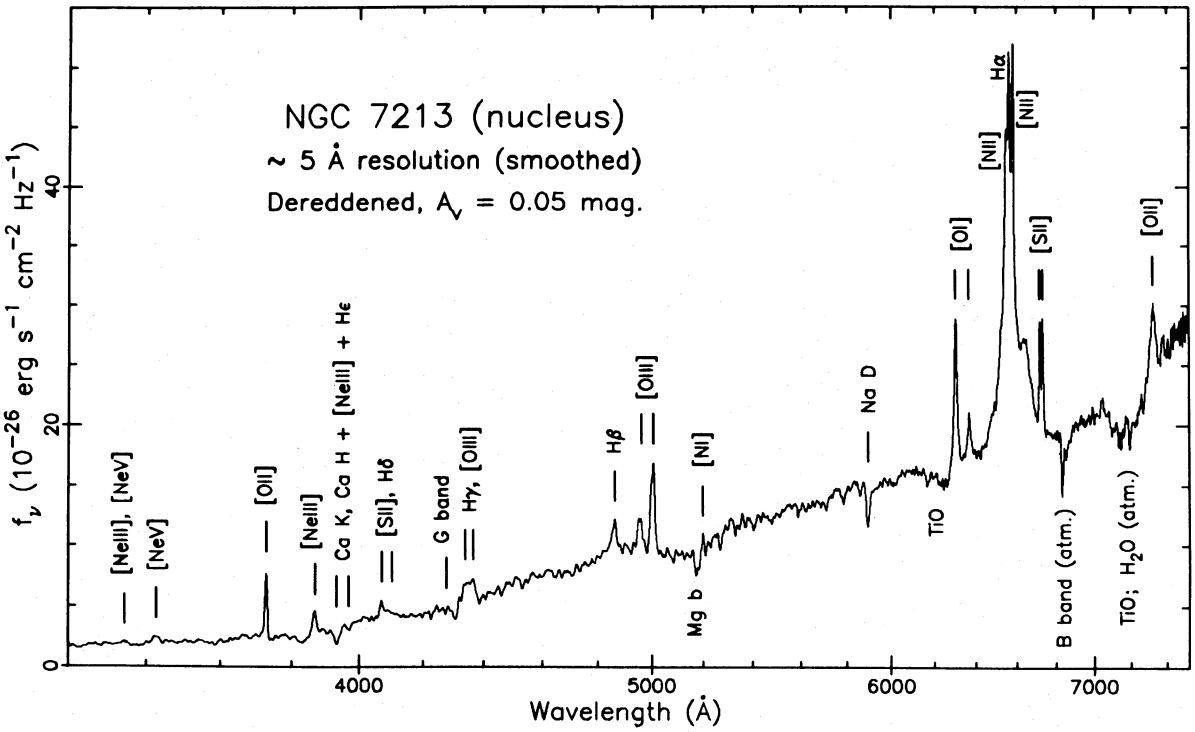

FIG. 1.—The dereddened optical spectrum of the central 2″ × 4″ of NGC 7213, smoothed with a 4.4 Å (FWHM) Gaussian, is shown on a logarithmic wavelength scale. As in all other spectra illustrated here, the systemic velocity of 1769 km s^{-1} was removed. Intensities are linear, but the absolute calibration is uncertain by ~ ±30%. Over the range ~λλ3700–6800 the S/N ratio is so high that most features are real.

through a long slit were not available, the starlight was removed by subtracting the spectrum of a different galaxy instead. IC 4889, the adopted template, is a bright $S0_{1/2}(5)$ galaxy (Sandage and Tammann 1981), and its spectral type, metallicity, and stellar velocity dispersion are quite similar to those in NGC 7213. Weak Hα, [N II] λλ6548, 6583, and [O II] λ3727 are the only emission lines visible.

Data were obtained at Las Campanas on 1983 August 13–14 UT in the manner used for NGC 7213, and a composite was formed from two separate spectra of the nucleus. Blueward of ~4500 Å the resolution (FWHM) is $\lesssim$2.5 Å in the composite, but redward the contribution of a second spectrum with $\lesssim$5 Å resolution is significant. Since the velocity dispersion in IC 4889 is roughly 200 km s^{-1}, the absorption lines are resolved in each individual spectrum, and the effective resolution is approximately uniform in the composite. The data were dereddened under the assumption that the Galaxy produces $A_v \sim$ 0.10 mag in the direction of IC 4889 (Burstein and Heiles 1982).

Although spectra of IC 4889 and NGC 7213 closely resemble each other, the apparent metallicity of the former is higher than that of the latter. This is partly due to the nonstellar component in NGC 7213 (Paper II), and comparable metallicities were found after its removal. To decrease remaining discrepancies, the flux in all pixels within a given section of IC 4889 was scaled by an appropriate amount, and a "featureless" component whose shape represents the absorption-free continuum was added or subtracted in order to bring the flux density back to the level of the true continuum. Thus, absorption lines in the modified spectrum had roughly the same equivalent width as corresponding lines in NGC 7213.

It was also necessary to adjust the continuum of IC 4889 so that its shape is nearly identical to that of NGC 7213. Differences may have been caused by subtracting an incorrect amount of nonstellar component from the spectrum of NGC 7213, or by incomplete removal of the reddening in either galaxy. The adjustment was made by (i) dividing the spectra into several sections of width ~400 Å, (ii) marking regions in both spectra where emission lines are present (or suspected to be present) in NGC 7213, (iii) fitting a quadratic or cubic to the unmarked points in each section, and (iv) rescaling the continuum of IC 4889 at every pixel with the local ratio of the two fits. The spectrum of the template was subsequently subtracted from that of the object. Since the same regions were excluded from the polynomial fits in both galaxies, and since the order of the fit in a given section was also the same, this approach was objective and produced a reliable removal of the stellar component. As a check, many regions devoid of emission were treated as though they actually do contain emission hidden among the numerous absorption lines, and no spurious features were discovered. Longward of ~5500 Å the signal-to-noise ratio of the template was not sufficiently high to be of great use in the subtraction.

Figure 2 illustrates the results. Emission lines only barely noticeable in the original spectrum rise prominently above the flat baseline. Excellent examples are [N I] λλ5198 + 5200, whose small width provides a striking contrast with [O III], and He II λ4686. Not only is the broad component of Hβ clearly visible, but a similar one is present in Hγ and possibly Hδ. There is no evidence of the Fe II emission often seen in Seyfert 1 galaxies (Phillips 1978). Noise in the net spectrum is somewhat greater than $2^{1/2}$ times that in either of the original spectra due to small differences in the velocity dispersion, metallicity, and spectral type of each galaxy.

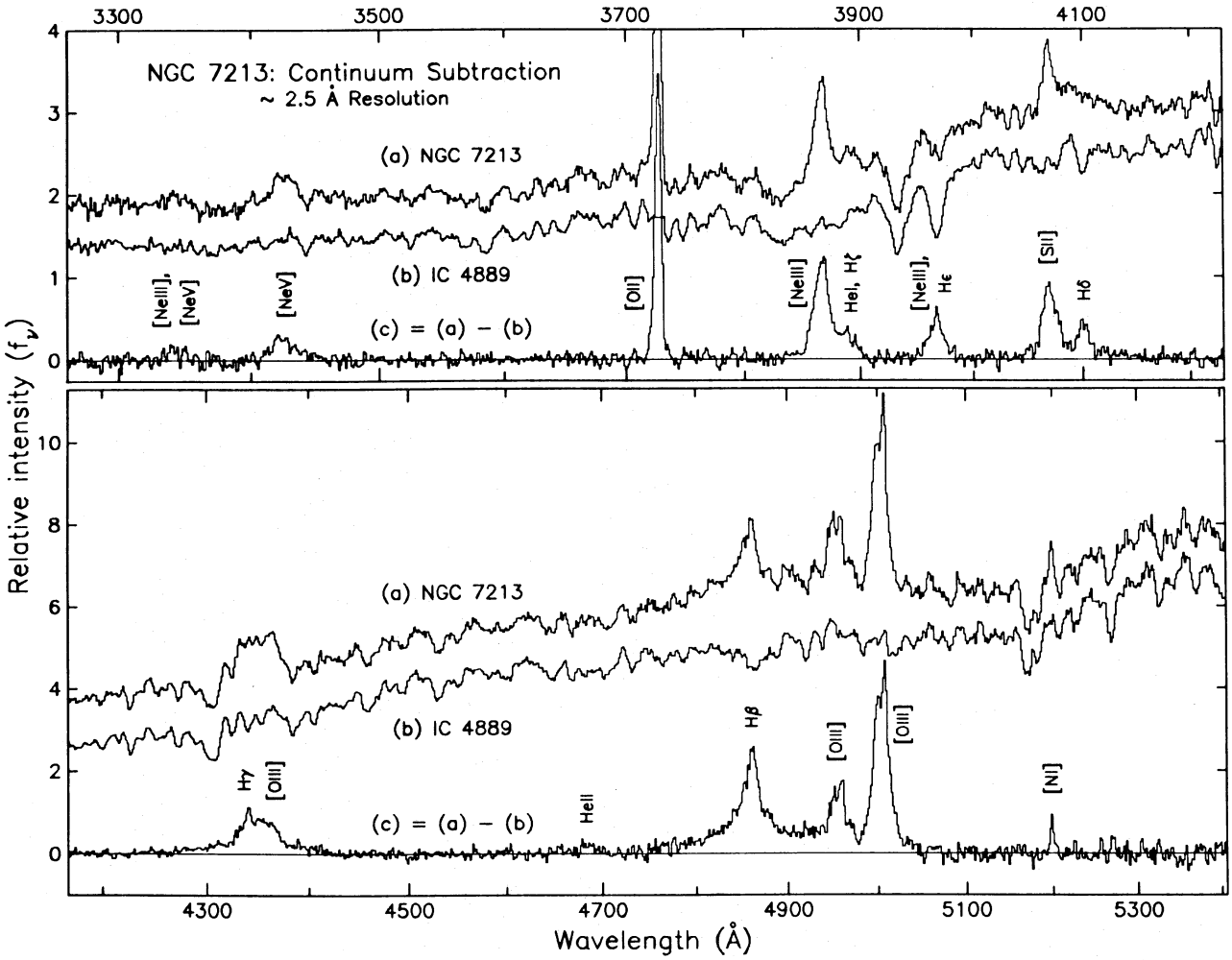

FIG. 2.—Spectra of (*a*) NGC 7213, (*b*) a template galaxy, and (*c*) the emission-line component of NGC 7213 obtained by subtracting (*b*) from (*a*) are plotted on a logarithmic wavelength (linear velocity) scale. All three spectra in each half are shown on the same ordinate scale, but the zero-point offsets differ to improve clarity, and the scale of the bottom half is twice that of the top. The nonstellar continuum is absent in (*a*), and the metallicity and general continuum shape of IC 4889 were adjusted to roughly match those of NGC 7213. The Galactic extinction ($A_v = 3.2E_{B-V} = 0.05$ mag) was removed in (*a*) and (*c*). [O II] λ3727 emission in IC 4889 was excised in (*b*).

b) Measurements of Emission Lines

Various parameters were measured from the net spectrum shown in Figure 2*c*, and from the red portion of the original spectrum. Wavelengths were determined by minimizing the absolute value of the convolution of each line with the derivative of a suitable Gaussian (Schneider and Young 1980). Since some emission lines (e.g., [O III] λ5007) exhibit weak, very narrow components in addition to broader blue wings, Gaussians having small dispersions were used to obtain accurate wavelengths for the peaks of lines, while larger dispersions gave better estimates of the line centroids. In all measurements the redshift of the galaxy ($v = 1769$ km s^{-1}), as given by Sandage and Tammann (1981), was removed. This systemic velocity is consistent with the value of 1789 km s^{-1} recently derived by cross-correlations of absorption-line spectra (Sadler 1984).

Intensities were obtained by integrating the flux in all pixels between the endpoints of each line. In many cases these were compared with values determined from the Gaussian which best approximates the given profile. For each line a weighted average based on an appraisal of the two methods was adopted. Full widths at half-maximum were also determined manually and from fits with symmetric functions, and are reasonably well defined. The full width at zero-intensity (FWZI), however, was usually measured less precisely, as it strongly depends on the signal-to-noise ratio in the wings of a line.

The results of various measurements are given in Table 1. Listed for each line is the laboratory wavelength, the difference between the laboratory wavelength and that of the line centroid, the difference between the laboratory wavelength and that of the line peak, the dereddened ($A_v = 0.05$ mag and $A_v = 0.61$ mag) intensity relative to I([O III] λ5007), the FWHM, the FWZI, and the number of km s^{-1} Å^{-1} at the line. Many of the quantities were derived by the use of special techniques discussed in the next section.

IV. DETAILED ANALYSIS OF BLENDS

a) [O I], [N II], Hα, [S II]

Figure 3*a* illustrates Hα and the remarkable differences in the widths and profiles of [O I] $\lambda\lambda$6300, 6364 and [S II] $\lambda\lambda$6716, 6731. The absence of emission from highly ionized Fe else-

TABLE 1

PROPERTIES OF EMISSION LINES IN NGC 7213

Line (1)	λ(1ab) (Å) (2)	$\Delta\lambda$(cen.) (Å) (3)	$\Delta\lambda$(peak) (Å) (4)	I/I(N2) ($A_v = 0.05$) (5)	I/I(N2) ($A_v = 0.61$) (6)	FWHM (Å) (7)	FWZI (Å) (8)	km s^{-1} Å^{-1} (9)
C IV	1549.5	...	...	6.80[a]	13.2[a]	...	...	193
C III]	1908.7	...	...	3.59[a]	6.93[a]	...	...	157
[Ne V]*	3345.83	−3.93[b]	...	0.046 ± 0.021	0.061	17.9 ± 4.5	46.0 ± 14.5	89.6
[Ne V]	3425.87	−1.27	...	0.142 ± 0.026	0.184	22.3 ± 2.6	61.9 ± 8.8	87.5
[O II]*	3726.05 +3728.80	−0.40[c]	0.08[c]	0.429 ± 0.011	0.516	7.1 ± 0.5	20.1 ± 2.5	80.4
[Ne III]	3868.76	−2.16	−0.46	0.342 ± 0.021	0.410	15.9 ± 0.9	50.1 ± 4.3	77.5
He I* +Hζ*	3888.65 3889.05	...[d]	...	0.091 ± 0.028	0.108	15.5 ± 2.0	45.0 ± 7	77.1
[Ne III]* +Hε*	3967.47 3970.07	...[e]	...	0.140 ± 0.026	0.164	17.3 ± 2.6	43.0 ± 10.6	75.6
[S II]*	4068.60 +4076.35	−0.70[f]	...	0.217 ± 0.022	0.251	17.0 ± 2.0	46.0 ± 7	73.7
Hδ*	4101.73	−1.61[g]	...	0.165 ± 0.066[h]	0.190	11.0 ± 3.0	24 ± 9	73.1
Hγ*	4340.46	−0.70[g]	0.40	0.516 ± 0.052[h]	0.571	25 ± 9	190 ± 40	69.1
[O III]*	4363.21	−4.21	...	0.203 ± 0.020	0.224	23.3 ± 3.6	67.0 ± 12	68.7
He II	4685.75	−0.95	...	0.064 ± 0.032	0.067	25.5 ± 6	63 ± 15	64.0
Hβ	4861.33	−1.43[g]	−0.33	1.435 ± 0.060[h]	1.462	28 ± 10	250 ± 40	61.7
[O III]	4958.92	−2.32	0.08	0.353 ± 0.020	0.355	20.5 ± 2.0	56.0 ± 8.4	60.5
[O III]	5006.85	−3.45	−0.05	1.000 ± 0.025	1.000	19.4 ± 1.0	64.9 ± 4.5	59.9
[N I]*	5197.94 +5200.41	−0.51[c]	...	0.044 ± 0.015	0.043	3.5 ± 0.8	11.0 ± 2	57.7
He I	5875.64	−0.7	...	<0.09[i]	<0.08[i]	15 ± 10	40 ± 25	51.0
[O I]	6300.32	−0.52	−0.12	0.825 ± 0.029	0.705	14.5 ± 1.1	59.9 ± 3.8	47.6
[O I]	6363.81	0.29	0.59	0.278 ± 0.019	0.236	13.8 ± 2.0	53.9 ± 7.0	47.1
[N II][j]*	6548.06	0.32	...	0.160 ± 0.024	0.133	7.2 ± 1.5	23.5 ± 4.6	45.8
Hα*	6562.79	0.21[k]	−0.19	9.04 ± 0.04[l]	7.50[l]	45 ± 20	420 ± 50	45.7
[N II]*	6583.39	0.32	...	0.479 ± 0.072	0.396	7.2 ± 1.5	23.5 ± 4.6	45.5
[S II]	6716.42	0.50	...	0.267 ± 0.006	0.218	7.4 ± 0.5	23.8 ± 1.3	44.6
[S II]	6730.78	0.22	...	0.269 ± 0.006	0.220	7.0 ± 0.5	22.9 ± 1.3	44.5
[O II]*	7319.1 +7330.2	−1.19[c]	...	0.371 ± 0.037	0.288	25.2 ± 2.9	65.0 ± 9.3	40.9

NOTES.—Col. (1), identification of species. Asterisks indicate major blends. Col. (2), lab wavelength, in air (vacuum λ for C IV, C III]). Bowen (1960) source of most lines. Col. (3), λ(observed centroid) − λ(lab). Typical error ~ ±0.5 Å, worse for weaker lines. Systemic velocity $v = 1769$ km s^{-1} removed. Col. (4), λ(observed peak) − λ(lab), given only if it differs significantly from col. (3). Col. (5), dereddened ($A_v = 0.05$ mag) flux relative to [O III] λ5007 ≡ N2 = 2.12×10^{-13} ergs s^{-1} cm^{-2}. Col. (6), dereddened ($A_v = 0.61$ mag) flux relative to [O III] λ5007 ≡ N2 = 3.77×10^{-13} ergs s^{-1} cm^{-2}. Relative errors similar to those in col. (5). Col. (7), full width at half-maximum (instrumental width removed). Col. (8), full width at zero intensity (instrumental width removed). Col. (9), km s^{-1} Å^{-1} at the given λ, for comparison of line widths and velocity shifts.

[a] Derived from Wu, Boggess, and Gull (1983).
[b] $\Delta\lambda$ calculated relative to [Ne V], but contamination by [Ne III] λ3342.5 possible.
[c] Close doublet. $\Delta\lambda$ calculated relative to average laboratory λ.
[d] He I badly blended with Hζ; uncertain relative strengths. $\Delta\lambda$ not calculated.
[e] [Ne III] blended with Hε; uncertain relative strengths. $\Delta\lambda$ not calculated.
[f] [S II] doublet unresolved. $\Delta\lambda$ relative to average lab λ, assuming $I(4069)/I(4076) = 4$.
[g] Refers to component with width comparable to that of [O III] λ5007.
[h] 20–25%, 20–25%, and ~40% of this total flux in Hβ, Hγ, and Hδ (respectively) is due only to the component described in note g.
[i] Upper limit—line may be detected, but large uncertainty.
[j] Parameters of [N II] λ6548 fixed relative to [N II] λ6583.
[k] Refers to Gaussian D in Table 2.
[l] Hα absorption removed to first order, but not with template galaxy IC 4889.

where in the spectrum argues against contamination of [O I] λ6364 by [Fe X] λ6374, and the similar profiles of [O I] λ6300 and [O I] λ6364 suggest that [S III] λ6312 is also not strong. Moreover, the relative intensity of the two [O I] lines agrees with theoretical predictions.

The continuum was artificially removed in Figure 3*b* by fitting cubic splines through selected points, since IC 4889 exhibits weak emission lines of Hα and [N II] $\lambda\lambda$6548, 6583. Absorption features such as the TiO band blueward of [O I] λ6300, the Ca + Fe line at ~λ6495, and the B band were excised, but no attempt was made to account for Hα absorption in NGC 7213. Gaussians were fitted to [S II] and subtracted from the spectrum, and the [O I] profiles were approximated with cubic splines. Figure 3*d* shows Hα after removal of [N II]. It was assumed that (i) I([N II] λ6583)/I([N II] λ6548) = 3.0, (ii) $\Delta\lambda = 35.4$ Å, and (iii) the lines are Gaussians whose width is equal to the average of the [S II] emission, as suggested by their appearance and by the expectation that roughly the same clouds produce these lines.

The narrow and broad components of Hα merge smoothly, and it is difficult to distinguish unambiguously between them. Two local maxima are visible, and the absence of strong absorption in this spectral region, together with the similar appearance of Hβ (Fig. 3*f*), makes it likely that the secondary peak is intrinsic to the profile. Figure 3*d* also illustrates the decomposition of the profile into six individual Gaussians (e.g.,

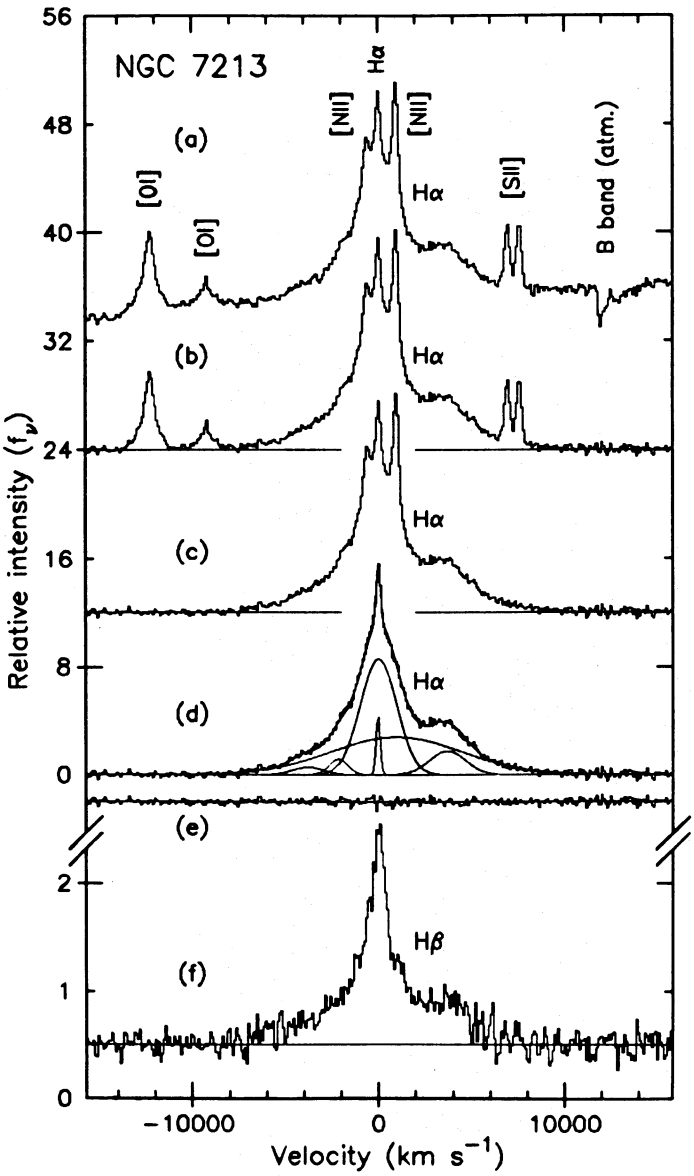

FIG. 3.—(*a*) The spectrum of NGC 7213 near Hα. In (*b*) the stellar continuum and obvious absorption lines (except Hα) are removed. Note the markedly different profiles of [O I] and [S II], which are removed in (*c*). [N II] is excised next (*d*), leaving only the asymmetrical Hα. A least-squares fit with the minimal number of Gaussians necessary to yield acceptable residuals (*e*) is also shown (see Table 2). Each of the six components cannot be physically significant, however, since the Hβ profile (*f*) has a narrower core.

Pelat and Alloin 1980, 1982). The overall fit is excellent (Fig. 3*e*), and the relevant parameters of each component are given in Table 2. The physical significance of all these Gaussians is questionable, however, since the FWHM of Hβ is noticeably smaller than that of Hα. If the decomposition of Hα is repeated with the physically reasonable requirement that one component resemble the core of Hβ, a total of seven Gaussians is necessary to produce a fit whose accuracy is comparable to that of the six-component fit. Failure to remove stellar Hα affects fluxes by only a few percent and does not change this result, as Balmer lines are generally weak in E and S0 galaxies. Thus, great physical significance should *not* be ascribed to all of the individual components. Only a few general conclusions, such as the existence of an asymmetrical broad component and the variation in Balmer decrement with velocity (Shuder 1982), can be drawn with confidence.

Some evidence for temporal variations may be found by comparing Figure 3 with previously published results. In particular, the "valley" visible in Hα and Hβ is not present in the spectrum taken by Phillips (1979) in 1978. This rather small change is well within the theoretically allowed variability, especially for such a low-luminosity active nucleus.

b) Hβ, [O III]

Inspection of Figures 1 and 2*a* suggests the presence of a broad Hβ component similar to that seen in Hα. Parameters of this line are difficult to measure due to prominent Mg *b* absorption, but subtraction of the template reveals a relatively clean profile.

Contamination of [O III] λ4959 was removed by fitting a cubic spline through points thought to represent the red wing of Hβ. The spline was required to vanish at the bottom of the "valley" between the [O III] lines (Fig. 2*c*) and to have a continuous first derivative. As a check, this technique produced I([O III] λ5007)/I([O III] λ4959) = 2.83, which is close to the theoretical prediction (2.96). In addition, the [O III] λ4959 and [O III] λ5007 profiles are remarkably similar: a narrow component is present at essentially the systemic velocity of 1769 km s^{-1}, but the bulk of the emission is blueshifted by ~180 km s^{-1}, as in many of the other forbidden lines.

c) [O III], Hγ

The blending caused by large intrinsic widths of Hγ and [O III] λ4363, together with the proximity of strong absorption (Fig. 4*a*), makes it difficult to measure the individual lines unless the underlying continuum is subtracted (as in Fig. 4*c*). A broad component of Hγ is visible, and a narrow "spike" appears as well. The former corresponds to those seen in Hα and Hβ, and the latter has a counterpart in Hα (Gaussian C in Table 2), but not in Hβ. A narrow component probably also exists in Hβ, but it is not visible due to an imperfect match between the strengths of Balmer absorption lines in NGC 7213 and IC 4889.

One of the most important diagnostics of physical conditions is [O III] λ4363. Estimates of its shape and intensity were obtained by assuming that the profiles of Hγ and Hβ are identical. Hβ was shifted so that its peak coincides with that of Hγ, and was subsequently scaled to produce the best overall fit to the broad component. An inherent assumption is that [O III] λ4363 does not have very extended wings that merge with those of Hγ. A scaling factor of 0.32 (Fig. 4*d*) produced a satis-

TABLE 2

PARAMETERS OF Hα DECOMPOSITION[a]

Gaussian	Relative Amplitude	λ (Å)	FWHM (Å)[b]	Flux[c] (10^{-14} ergs s^{-1} cm^{-2})
A	1.00	6481	42.4	4.21
B	2.07	6516.5	25.9	5.27
C	7.81	6562.6	5.65	4.27
D	15.0	6563	50.6	73.6
E	4.91	6585	184	86.8
F	3.14	6645	50.6	15.0

[a] See Fig. 3*d*.
[b] Instrumental resolution (FWHM ~ 2.5 Å) not removed.
[c] Dereddened, A_v = 0.05 mag.

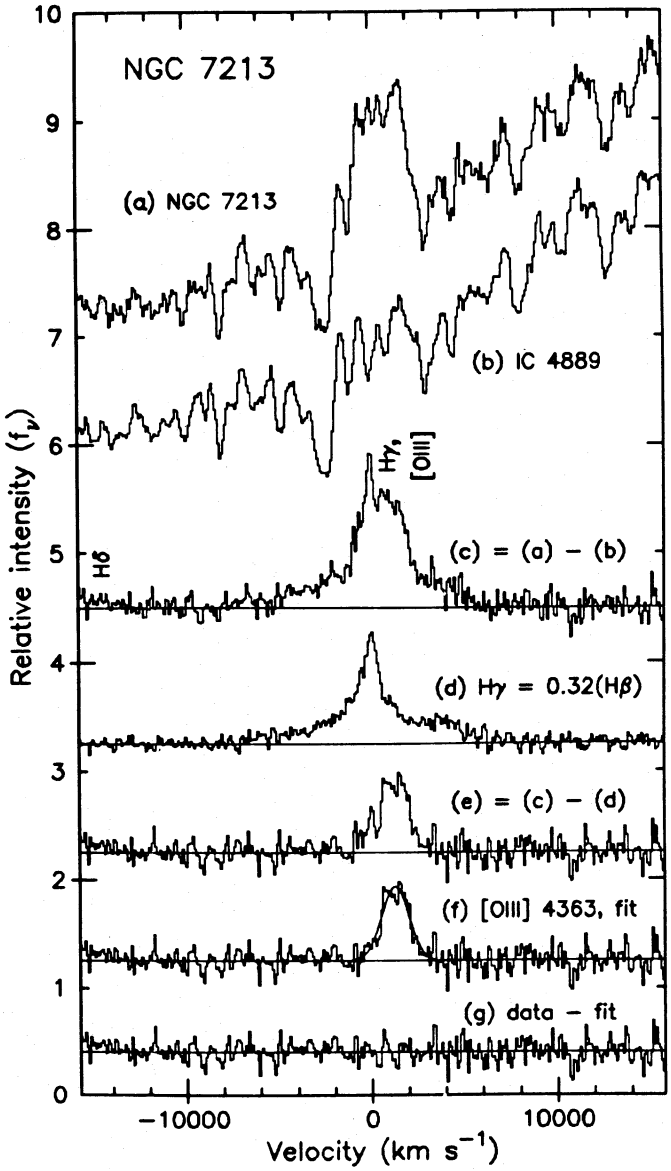

FIG. 4.—Spectra (*a*), (*b*), and (*c*) represent a small section of Fig. 2. [O III] λ4363 and Hγ are blended in (*a*), and are contaminated by absorption lines. The template galaxy (*b*) is drawn on the same relative intensity scale but offset for clarity. It is subtracted from NGC 7213 in (*c*), revealing the presence of broad Hγ emission that has a close counterpart in the Hβ profile (*d*). Hβ is scaled so that the red and blue wings match those of Hγ, and in (*e*) it is subtracted from the blend. What remains is largely [O III] λ4363, but a small, narrow Hγ line is also visible. After removing the remaining Hγ (*f*), a Gaussian is fitted to [O III] λ4363. The approximation is satisfactory, as shown by the residuals (*g*).

factory fit and leads one to believe that the profiles of Hγ and Hβ are very similar. In Figure 4*e*, Hγ was subtracted from the blended line, leaving [O III] λ4363 and a small residual of narrow Hγ emission which was removed in Figure 4*f*.

Table 1 shows that [O III] λ4363 is remarkably strong and also somewhat broader than the related [O III] λλ4959, 5007 lines. These measurements play an important role in subsequent discussions, and it must be stressed that they were probably not overestimated. It is likely, however, that the derived strength of [O III] λ4363 was too large in a number of previous studies of Liners, since Figure 4*b* clearly demonstrates a high point in the normal stellar continuum precisely at the position expected for [O III] λ4363. Failure to properly account for the underlying stellar absorption lines therefore leads to serious errors in the measured flux of [O III] λ4363, as emphasized by Keel and Miller (1983) and by Rose and Tripicco (1984).

d) [S II], Hδ, [Ne III], Hε

A puzzling blend composed of [S II] λλ4069, 4076 and Hδ is seen in Figure 5*a*. There is no clear separation between [S II] and the extended red wing, whose centroid appears ~10–15 Å blueward of its expected position if it is Hδ. Weak [Fe V]

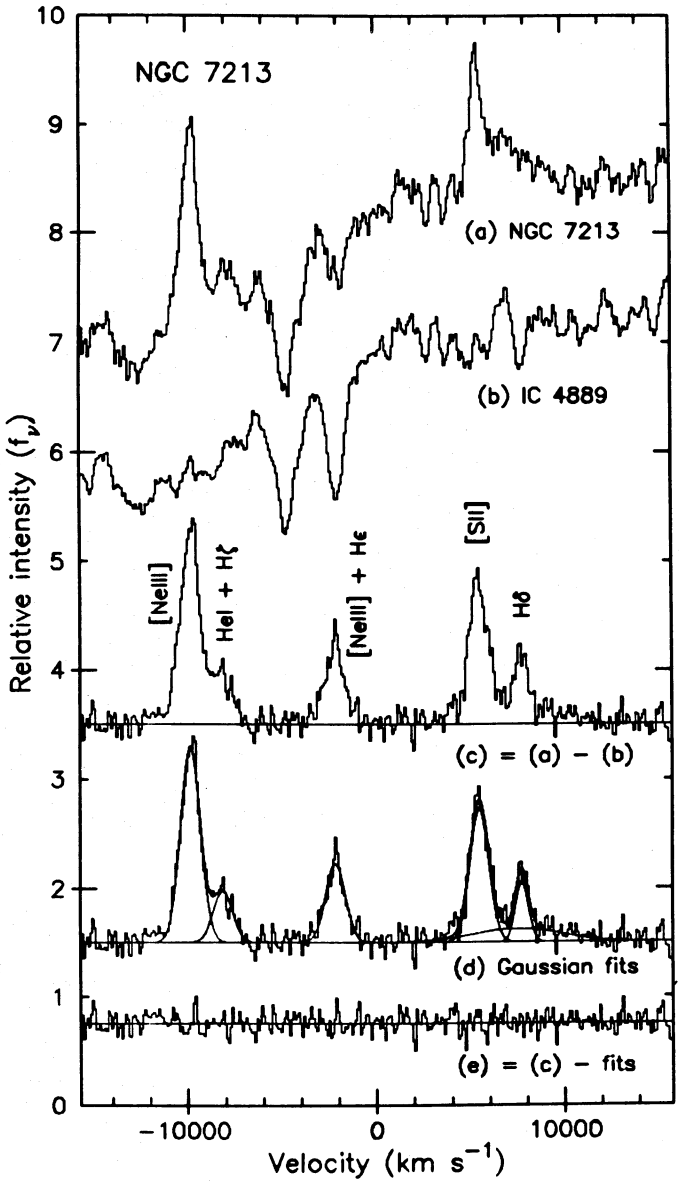

FIG. 5.—The top three spectra represent a portion of Fig. 2. Strong absorption lines preclude accurate measurement of most emission in NGC 7213 (*a*), but IC 4889 (*b*) provides a close approximation to the stellar component. The net emission-line spectrum of NGC 7213 (*c*) reveals the [Ne III] λ3967 + Hε blend, which was previously hidden by Ca II H absorption. Similarly, although a high point in the stellar continuum blends [S II] λλ4069 + 4076 and Hδ in (*a*), the emission lines are well resolved in (*c*), and a broad component of Hδ is visible as well. Gaussians (*d*) are used to represent the emission lines, leaving very small residuals (*e*).

λ4071.5 might be present, but this is improbable in view of the absence of additional Fe lines having comparable strength (Osterbrock 1981).

The puzzle disappears when the stellar component, which contains a high point at $\sim\lambda$4088, is subtracted from NGC 7213. The blend breaks up into several recognizable lines: [S II] λ4069, an Hδ line of comparable width, and a very weak, poorly determined broad component of Hδ which corresponds to the wings seen in Hα, Hβ, and Hγ. The lines can be fitted well by Gaussians. Of course, a portion of the [S II] profile is due to emission at λ4076, which is calculated to be a factor of $\sim$4 weaker than [S II] λ4069.

Figure 5*a* also shows how [Ne III] λ3967 and Hϵ are hidden in the strong Ca II H (λ3968) absorption line. There is a hint of He I λ3889 + Hζ emission redward of [Ne III] λ3869 as well, and these weak lines are clearly visible in Figure 5*c*. The derived strength of [Ne III] λ3967 is roughly 0.30 that of [Ne III] λ3869, in agreement with theory. A broad component of Hϵ is probably present, but its small flux cannot be measured due to comparable uncertainties in the procedure used to remove the stellar component from this troublesome spectral region.

V. INTERPRETATION OF THE EMISSION LINES

To investigate the ionization mechanism in NGC 7213, it is necessary to disentangle physically distinct regions by examining the various widths and intensity ratios in Table 1; otherwise, conclusions drawn from the data may be invalid. With this in mind, the relevant electron densities and temperatures are now determined. Unless otherwise stated, all line intensities are dereddened with the Galactic extinction $A_v = 0.05$ mag, since the value of 0.61 mag derived from an analysis of the optical continuum may be inconsistent with the X-ray measurements (Paper II).

a) Atomic Data

Theoretical emission-line intensity ratios were calculated as a function of n_e and T_e using detailed balance in ions having five low-lying levels in the ground state configuration (Kafatos and Lynch 1980). Temperature-dependent collision strengths from the following sources were used: Péquignot and Aldrovandi (1976) for [O I], Pradhan (1976, 1978) for [O II] and [S II], Baluja, Burke, and Kingston (1981) for [O III], Seaton (1975) for [N II], Pradhan (1974) for [Ne III], and Giles (1979) for [Ne V]. Sources for the transition probabilities were Garstang (1968) for [O I] and [Ne III], Nussbaumer and Rusca (1979) for [N II] and [Ne V], Nussbaumer and Storey (1981) for [O III], Mendoza and Zeippen (1982) for [S II], and Zeippen (1982) for [O II].

The critical density n_e^i(crit) for each level i, above which collisional de-excitation of the level is important (Osterbrock 1974), was calculated from

$$n_e^i(\text{crit}) = \sum_{j<i} A_{ij} \Big/ \sum_{j\neq i} q_{ij} \,, \qquad (1)$$

where A_{ij} is the transition probability (from level i to level j) and q_{ij} is the collisional (de)excitation rate.

b) Line Widths

Table 1 demonstrates that the forbidden lines in NGC 7213 display a great range in width. An impressive example is provided by [O II] $\lambda\lambda$3726, 3729 and [O II] $\lambda\lambda$7319, 7330, which show that lines from the *same species* receive different relative contributions from various clouds. The same can be said for [S II] $\lambda\lambda$6716, 6731 and [S II] $\lambda\lambda$4069, 4076, as well as for [O III] $\lambda\lambda$4959, 5007 and [O III] λ4363. This obviously complicates the derivation of densities, temperatures, and reddenings from emission-line intensity ratios.

Line width increases systematically with the ionization potential (χ) of the corresponding ion in a few active galaxies (e.g., Osterbrock 1981; Pelat, Alloin, and Fosbury 1981). An increase in the gas excitation level and cloud velocities with decreasing distance from the central source of ionizing radiation is the probable cause of this. Although such a correlation also appears to be present in NGC 7213 (Fig. 6), lines from the same species but with markedly different widths suggest that χ is *not* the fundamental parameter. Rather, a physical variable which in many cases increases with χ, but is also able to distinguish between transitions from different upper levels in a given species, would be better.

A parameter satisfying these requirements is the critical density. Indeed, Figure 7 illustrates the close relationship between the width of a forbidden line and n_e(crit) for the upper level from which the corresponding electron transition occurs. Lines associated with n_e(crit) $\sim 10^6$ cm^{-3} are broader than those having small ($\sim 10^3$ cm^{-3}) values, and both the FWHM and FWZI obey the same relation [$v \propto n_e(\text{crit})^{1/5}$], obtained with unweighted linear least-squares fits. Since there are few points at low n_e(crit), several of which are associated with large errors, a weighted analysis essentially uses only the points at high n_e(crit) and gives a linear fit which is less plausible than an unweighted one. Balmer lines are not plotted because the effects of radiative transfer greatly complicate the interpretation of n_e(crit), but it is obvious from Table 1 that the observed general trend continues if $n_e \sim 10^9$ cm^{-3} is assumed for the broadest components.

Most of the scatter in Figure 6 is absent in Figure 7, and the final correlation coefficients (r) of the fits are $\sim$0.73 and $\sim$0.92, respectively. As usual, $r = 1.0$ represents a perfect correlation, whereas $r = 0.0$ for completely uncorrelated data. It is possible that for a given value of n_e(crit) the average width of lines produced by species having high χ (e.g., [Ne V], [O III]) is slightly greater than that of lines from species with low χ, but the number of lines is not sufficiently high to allow a statistically significant conclusion. Thus, in NGC 7213 the *critical density is clearly the primary discriminant*, while χ has only secondary importance.

Pelat, Alloin, and Fosbury (1981) suggested that the forbidden lines in the Seyfert galaxy NGC 3783 may obey a similar relationship between n_e(crit) and width, but they did not measure lines produced by low-ionization species having large critical density (such as [O I] $\lambda\lambda$6300, 6364, [S II] $\lambda\lambda$4069, 4076, and [O II] $\lambda\lambda$7319, 7330). Instead, every line in their sample associated with a large n_e(crit) is also characterized by high χ, and similarly for low values of and n_e(crit). Hence, the correlation they obtained between width and χ was roughly as strong as that obtained between width and n_e(crit), and it was not clear which of the two parameters is fundamental.

The emissivity of gas (per unit volume) is proportional to n_e^2 below n_e(crit) and to n_e above it. Thus, a given line is emitted most efficiently from gas whose density is close to n_e(crit), so emission lines can act as tracers of n_e if the range is sufficiently large. Figure 7 implies that *many clouds with different bulk motions and densities exist in the narrow-line region of NGC*

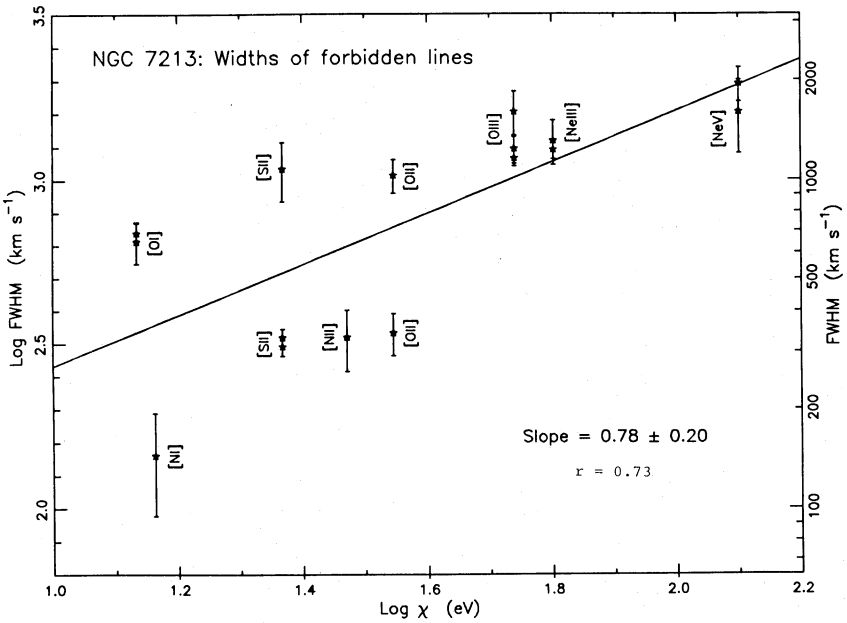

FIG. 6.—Log FWHM is plotted against log χ for each forbidden line, where χ is the ionization potential of the corresponding species. Widths and errors are taken from Table 1. An unweighted linear least-squares fit formally indicates the presence of a correlation (correlation coefficient $r = 0.73$). Several lines from the same species but with markedly different widths (e.g., [O II], [S II]), however, demonstrate that *the correlation is not of fundamental significance*, and that χ is at most a secondary parameter.

7213. Dense clouds appear to be moving the fastest, although it is not known *a priori* whether this motion is turbulent or systematic.

Of course, the existence of distinct regions having widely different densities and velocities has long been accepted as the explanation for the presence of narrow forbidden and permitted lines, together with broad permitted lines, in the spectra of Seyfert nuclei. It is reasonable that in at least some galaxies substantial density variations also exist among clouds which produce the narrow components. In fact, forbidden lines of unequal width have been noticed in a number of Liners and radio galaxies (Heckman 1980; Danziger, Fosbury, and Penston 1977), but NGC 7213 is the first example in which lines arising from the *same species* are significantly different.

c) *Physical Conditions*

The widths can be used to distinguish between different clouds. [O II] $\lambda\lambda$3726, 3729 and [S II] $\lambda\lambda$6716, 6731 are compa-

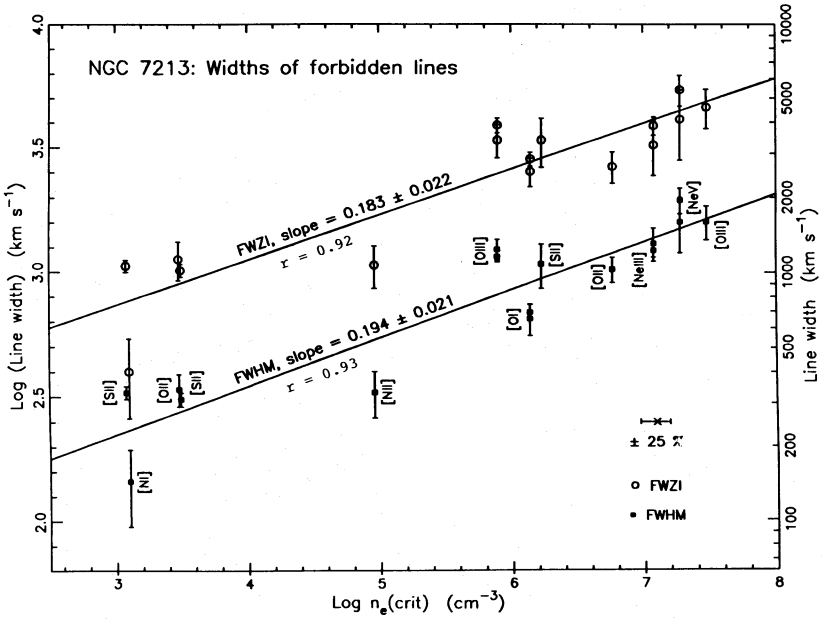

FIG. 7.—Log FWHM (*filled squares*) and log FWZI (*open circles*) are plotted against log n_e(crit) for each forbidden line, where n_e(crit) is the critical density of the upper level from which the corresponding transition occurs. Widths and errors are taken from Table 1, and uncertainties in theoretically calculated critical densities may be of order $\pm 25\%$ (*horizontal bar*). Unlike Fig. 6, in which there is considerable scatter, the least-squares fits indicate very high correlation coefficients ($r \sim 0.92$). Note that lines from the same species but with markedly different widths strengthen the correlation. Since gas emits a line most efficiently when it is near n_e(crit) for that line, clouds with *different* bulk motions and densities must exist in the narrow-line region.

rable in width, so they probably arise from roughly the same gas. If $T_e = 10^4$ K, the observed ratio $I([\text{S II}]\ \lambda6716)/I([\text{S II}]\ \lambda6731) = 0.99 \pm 0.03$ corresponds to $n_e \sim 470 \pm 60$ cm^{-3}, in which case $I([\text{O II}]\ \lambda3726)/I([\text{O II}]\ \lambda3729)$ is predicted to be $\sim 0.97 \pm 0.04$. Although the [O II] doublet is unresolved, this value is consistent with its symmetrical profile. Densities which differ greatly from ~ 500 cm^{-3} are excluded—the intensity ratio is ~ 0.74 when $n_e = 100$ cm^{-3} and ~ 1.23 when $n_e = 1000$ cm^{-3}, and the [O II] profile should then be noticeably asymmetrical.

Clouds which give rise to the narrow "nebular" doublets ([O II] $\lambda\lambda$3726, 3729 and [S II] $\lambda\lambda$6716, 6731) cannot possibly produce the "auroral" ([O II] $\lambda\lambda$7319, 7330) and "transauroral" ([S II] $\lambda\lambda$4069, 4076) lines simultaneously, as shown in Figure 8 for [O II]. The two blends are drawn on the same velocity scale and are decomposed into their two major constituents (each having the same width), under the assumptions that $I([\text{O II}]\ \lambda7319)/I([\text{O II}]\ \lambda7330) = 1.27$ and $I([\text{O II}]\ \lambda3726)/I([\text{O II}]\ \lambda3729) = 1.00$. The former ratio is almost completely independent of n_e and T_e, whereas the latter represents the best fit to the data and is consistent with the ratio 0.97 ± 0.04 derived above. Clearly, the components of the nebular doublet are considerably narrower than the individual auroral lines, and therefore cannot be produced by the same ions.

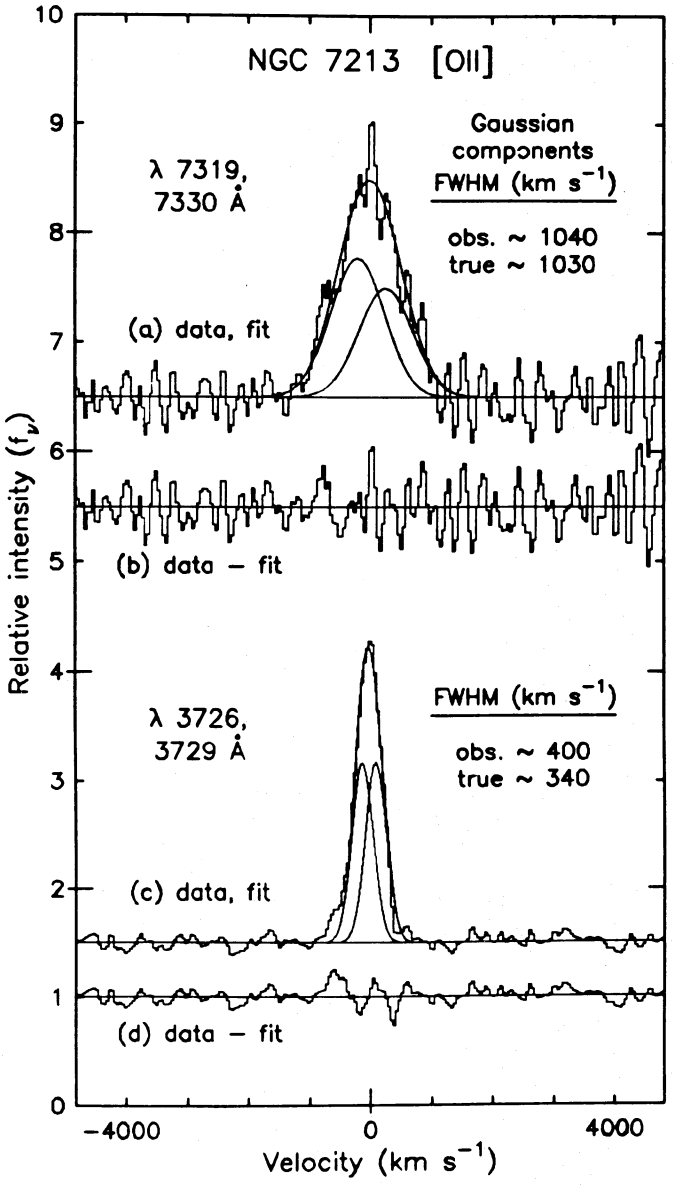

FIG. 8.—[O II] $\lambda\lambda$7319 + 7330 (*a*) and [O II] $\lambda\lambda$3726 + 3729 (*c*) are plotted on the same velocity and relative intensity scales. The blends are decomposed into their two major constituents, each having the same width. The true width of a line is obtained by removing the instrumental resolution from the observed width. Components of the blue doublet are considerably narrower than the individual red lines, and cannot be produced by the same clouds.

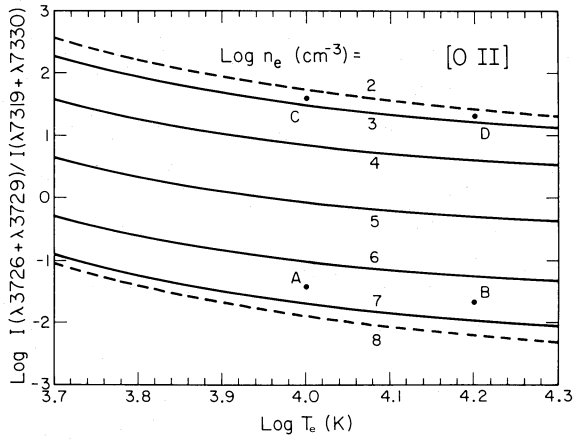

FIG. 9.—The logarithm of the theoretical intensity ratio of nebular to auroral [O II] emission ($A_v = 0.0$) is plotted as a function of log T_e for a range of densities. Dashed lines represent the low- and high-density limits. Points A and B show that the intensity of broad [O II] $\lambda\lambda$3726, 3729 lines from clouds which give rise to the broad auroral lines in NGC 7213 is negligible at reasonable temperatures. Similarly, points C and D indicate that the narrow components of [O II] $\lambda\lambda$7319, 7330 should be difficult to detect.

If the broad [O II] $\lambda\lambda$7319, 7330 lines are produced by gas near its critical density ($\sim 5.9 \times 10^6$ cm^{-3}), then Figure 9 shows that the corresponding components of [O II] $\lambda\lambda$3726, 3729 should be a factor of ~ 26 less intense if log $T_e = 4.0$ (point A),[1] and ~ 47 times weaker if log $T_e = 4.2$ (point B), assuming $A_v = 0.0$ mag. The absence of this broad component in Figure 8*c* is therefore not surprising. Similarly, if the narrow nebular emission is produced in gas with $n_e \sim 470$ cm^{-3}, then the flux of this line should be ~ 40 times greater than that of the corresponding narrow [O II] $\lambda\lambda$7319, 7330 if log $T_e = 4.0$ (point C), and a factor of ~ 20 greater if log $T_e = 4.2$ (point D). This component is difficult to detect in Figure 8*a* due to the low signal-to-noise ratio, but the top half of the profile may be slightly too narrow in comparison with the bottom half and the Gaussian fit.

The same reasoning applies to [S II]. If the broad transauroral lines are produced by gas near n_e(crit) $\sim 1.7 \times 10^6$ cm^{-3}, the corresponding components of [S II] $\lambda\lambda$6716, 6731 should be factors of ~ 33 and ~ 48 weaker ($A_v = 0.0$) if log $T_e = 4.0$ and log $T_e = 4.2$, respectively (Fig. 10), and are undetectable in Figure 3*b*. Moreover, if the narrow nebular doublet is produced by gas with $n_e \sim 470$ cm^{-3}, then its strength should be ~ 12 times greater than the narrow component of the transauroral lines if log $T_e = 4.0$ and a factor of ~ 7 greater if log $T_e = 4.2$. Nonzero reddening would lead to even larger factors. Figure 5 indicates that [S II] $\lambda4069$ might have a very small narrow core, but this cannot be established with certainty.

Of course, if substantial quantities of gas exist at densities *between* 10^3 cm^{-3} and 10^6 cm^{-3}, one should expect to see

[1] Note that log here and throughout is log base 10.

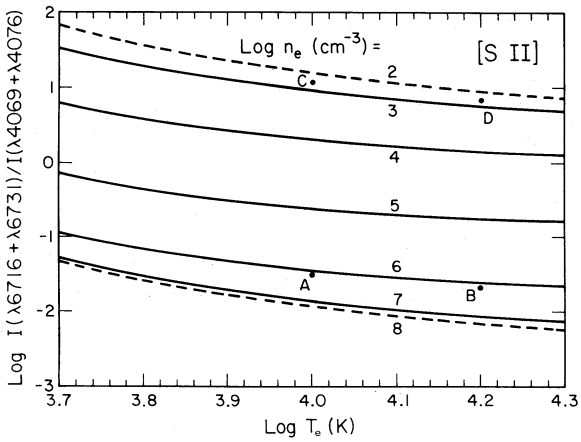

FIG. 10.—The theoretical ratio of nebular to transauroral [S II] emission ($A_v = 0.0$) is plotted in the same manner as in Fig. 9, and the interpretation of points A, B, C, and D is similar as well.

many components of various widths in the profile of a given line. In practice, these usually cannot be distinguished because they blend with one another and have roughly the same profile. A superposition of components with different widths and intensities is probably present in [O I] λλ6300, 6364, however, as Figure 3*b* shows that the wings are much more extended than those in a single Gaussian.

Additional evidence for the presence of densities $\gtrsim 10^6$ cm^{-3} is found from careful examination of the nebular [O III] λλ4959, 5007 and auroral [O III] λ4363 lines. Assume for the time being that all of the [O III] lines originate in the same clouds. Then a density estimate for the O^{++} zone can be obtained from the ratio $R \equiv I$([O III] λλ4959 + 5007)/I([O III] λ4363), even though this is normally used as a measure of the temperature (Osterbrock 1974). Indeed, Figure 11 shows that

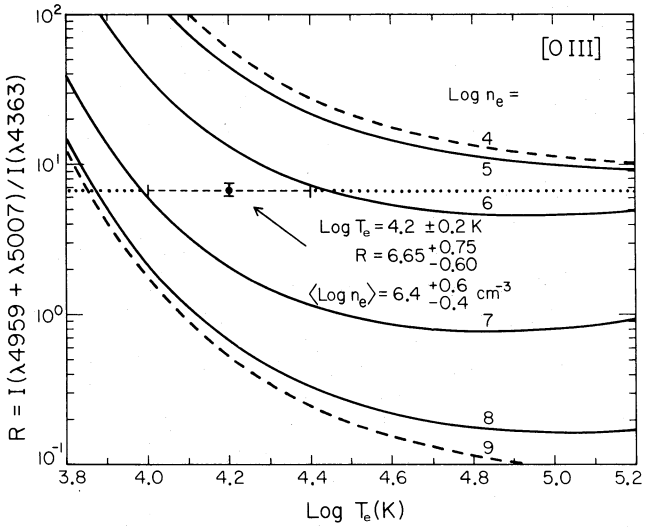

FIG. 11.—The theoretical intensity ratio of nebular to auroral [O III] emission (R) is plotted as a function of log T_e for a range of densities and zero reddening. Dashed lines approximate the low- and high-density limits. In NGC 7213, the observed value $R = 6.65$ cannot be produced *at any temperature* unless $n_e \gtrsim 10^{5.5}$ cm^{-3} in clouds which produce the [O III] emission. At $T \sim 16{,}000$ K, the average density is $\sim 10^{6.4}$ cm^{-3}; the true values are probably $\gtrsim 10^7$ cm^{-3} and $\lesssim 10^6$ cm^{-3} in regions which produce most of the auroral and nebular lines, respectively. The average density can vary between 10^6 and 10^7 cm^{-3} for the large range $4.0 \leq \log T_e \leq 4.4$.

the observed value ($R = 6.65$) cannot be achieved unless n_e is at least $\sim 10^{5.5}$ cm^{-3}, *for any reasonable temperature*. Within the range $10{,}000 \leq T_e \leq 25{,}000$ K ($4.0 \leq \log T_e \leq 4.4$) the density must be between 10^6 and 10^7 cm^{-3}. If $T_e = 16{,}000$ K ($\log T = 4.2$), which is near the high end in Seyfert galaxies (Koski 1978), then $n_e = 10^{6.4}$ cm^{-3}. The derived density becomes still *higher* if relative intensities of emission lines are corrected with $A_v = 0.61$ mag, as suggested by the continuum decomposition (Paper II). This startling result clearly demonstrates that enormous differences in density must exist in the forbidden-line gas of NGC 7213.

Similar arguments could be applied to [N II] λ5755 and [O I] λ5577, but these nondetections do not provide useful additional constraints on n_e and T_e. The situation could change if an absorption template were accurately subtracted from this spectral region.

It is important to mention that high n_e in the O^{++} zone exists in several broad-line radio galaxies (Osterbrock, Koski, and Phillips 1976) and low-redshift QSOs (Baldwin 1975): the small values of R in 3C 390.3, 3C 382, PKS 0837 − 12, and PKS 1217 + 02 indicate that $n_e \gtrsim 10^6$ cm^{-3}. These galaxies are cases of extreme activity, and their Balmer lines are generally broader than those in classical type 1 Seyferts. There has previously been no conclusive evidence that such large densities are also found in the narrow-line regions of less luminous Seyferts or in Liners, however. The observed ratios log {I([O III] λλ4959 + 5007)/I([Ne III] λλ3869 + 3967)} = 0.47 and log R = 0.82, for example, place NGC 7213 in the lower left corner of Figure 1 in Heckman and Balick (1979), suggesting $n_e \sim 10^{6.6}$ cm^{-3} and $T_e \sim 13{,}000$ K. Almost all other objects in Figure 1 have a lower density, and the two exceptions are peculiar in that the derived T_e seems unreasonably low ($T_e \lesssim$ 7500 K). Note that Ferland and Netzer (1983) had dismissed the possibility of high densities in the emission-line gas of Liners.

The density estimate for the O^{++} zone was made under the assumption that all three of the [O III] lines are produced in the same clouds, but Table 1 and Figure 7 show that [O III] λ4363 is slightly *broader* than the nebular lines. Since regions with $n_e \sim 10^7$ cm^{-3} produce more [O III] λ4363 [n_e(crit) $\sim 3 \times 10^7$ cm^{-3}] relative to [O III] λλ4959, 5007 [n_e(crit) $\sim 7.9 \times 10^5$ cm^{-3}] than those with $n_e \sim 10^6$ cm^{-3}, a single value of the density cannot, strictly speaking, be obtained from the observed ratio R. The quoted value of $10^{6.4}$ cm^{-3} is biased toward high densities, and a more reasonable interpretation is that $n_e \gtrsim 10^7$ cm^{-3} in clouds which produce most of the auroral line, while $n_e \lesssim 10^6$ cm^{-3} in those from which a majority of the nebular emission arises. Calculations indicate that the charge-exchange reaction $H^0 + O^{+3} \rightarrow H^+ + O^{++}$, which can enhance [O III] λ4363 (Butler, Heil, and Dalgarno 1980; Dalgarno and Sternberg 1982), probably does not seriously affect these conclusions.

The existence of a region with $n_e \gtrsim 10^7$ cm^{-3} (as for [O III] λ4363) implies that Balmer emission should be enhanced relative to [O III] λλ4959, 5007 in NGC 7213 (Péquignot 1984). This occurs because n_e is considerably greater than n_e(crit) for [O III] λλ4959, 5007. Thus, while Balmer emission is proportional to n_e^2 at $n_e \sim 10^7$ cm^{-3}, nebular [O III] is proportional only to n_e, so the former should be stronger relative to the latter than in the low-density ($n_e \sim 10^3$–10^5 cm^{-3}) clouds normally found in the narrow-line regions of active galactic nuclei. Figure 2*c* shows that this is true in NGC 7213: [O III] λλ4959 + 5007 is roughly a factor of 4.4 stronger than

the corresponding component of Hβ, noticeably smaller than the value of 10–20 generally found in Seyfert 2 galaxies (Koski 1978) and in the narrow-line regions of type 1 Seyferts. Of course, part of this decrease in [O III] is also due to the low ionization parameter generally associated with Liners.

These results unambiguously demonstrate that large density variations among clouds of gas in the narrow-line region of NGC 7213 play an important role in determining the emission-line spectrum, and it is inferred that other galaxies, such as NGC 1052 (Keel and Miller 1983), might be similarly affected. Lines of a given element which arise from different stages of ionization may not necessarily be directly compared in photoionization and shock models, and in classification schemes (e.g., Heckman 1980; Baldwin, Phillips, and Terlevich 1981). Even different lines produced by the *same* ion can originate in regions having substantially different physical conditions. Evidence for this based on relative intensities has been presented in several previous investigations (e.g., Heckman and Balick 1979), but NGC 7213 is by far the most convincing case to date since it also exhibits a variety of profiles. Thus, one must exhibit caution when deducing physical parameters such as reddening (Malkan 1983*a*), density, and temperature. It is also not a simple task to use the line strengths in photoionization models, since most of these are too simplistic (e.g., constant density or pressure) to allow for the different observed conditions in NGC 7213.

d) Geometry and Kinematics

In NGC 7213, line widths are correlated primarily with the density rather than with the ionization state. Such a situation can arise if individual clouds of differing densities are all optically thick to Lyman continuum radiation, since several different stages of ionization are represented in each cloud.

If clouds move freely in the potential well of a massive central object, and if they are in pressure equilibrium with a hot confining medium (§ VII*a*), then the densest ones should be closest to the nucleus and have the greatest velocities. Figure 7 and the measured wavelengths of emission lines are consistent with this, but dust must be present in the clouds to provide selective obscuration. In particular, narrow lines such as [S II] λλ6716, 6731, as well as the very weak, narrow components of broader lines (e.g., [O III] λλ4959, 5007) share the systemic (absorption line) velocity of NGC 7213, whereas Table 1 shows that the broad components of forbidden lines (especially those associated with high ionization potentials) are systematically blueshifted. One interpretation is that the dense clouds have substantial radial motions. Suppose that dust survives in the neutral and singly ionized zones, but not in the hot regions where [Ne III], [O III], and [Ne V] are produced. The high-ionization lines will be seen preferentially from the illuminated faces of clouds beyond the continuum source. If most of the clouds are approaching the nucleus or emit primarily during the inward leg of a Keplerian orbit (as in the model of Carroll and Kwan 1983: § VII), then the high-ionization lines will be blueshifted. [O I], on the other hand, which is produced throughout the neutral, dusty region will have no preferred direction. Lines of [O II] and [S II] may or may not exhibit net blueshifts, depending on the distribution of dust and on the cloud kinematics; in NGC 7213, the auroral and transauroral components are slightly blueshifted, while the nebular ones are not, emphasizing once again that not all lines are emitted from the same clouds (§ V*c*). It is also possible that the narrow peaks of emission lines, including those of [O III] mentioned above, might be produced in a "reservoir" of low-density gas which is far from the nucleus, moves rather slowly, and does not suffer from as much obscuration by dust.

e) The Balmer Decrement

It is not possible to obtain separate Balmer decrements for each of the Gaussian components of Hα in Figure 3*e*. The flux within the entire profile of a Balmer line is therefore computed, with the exception of the very narrowest component of Hα (Gaussian C in Table 2) and Hγ (the "spike" in Fig. 4*c*). The observed decrement (Galactic $A_v = 0.05$ mag removed) is

$$I(\mathrm{H}\alpha)/I(\mathrm{H}\beta)/I(\mathrm{H}\gamma)/I(\mathrm{H}\delta) = 6.20/1.00/0.35/0.12 .$$

If the Balmer lines are produced purely by recombination, then at an average density of 10^7 cm^{-3} and a temperature of 1.5×10^4 K the Case B decrement should be (Brocklehurst 1971)

$$I(\mathrm{H}\alpha)/I(\mathrm{H}\beta)/I(\mathrm{H}\gamma)/I(\mathrm{H}\delta) = 2.76/1.00/0.47/0.26 ,$$

which differs significantly from the observed one. A standard assumption is that dust reddens the lines, in which case $I(\mathrm{H}\alpha)/I(\mathrm{H}\beta)$, $I(\mathrm{H}\gamma)/I(\mathrm{H}\beta)$, and $I(\mathrm{H}\delta)/I(\mathrm{H}\beta)$ imply $A_v \sim 2.2$, 2.0, and 3.5 mag, respectively. The last of these is very uncertain due to the weakness of Hδ, but the first two show good agreement, so $A_v = 2.1$ mag is adopted. This exceeds the value $A_v = 0.61$ mag obtained for the continuum. Such a discrepancy is common, particularly in broad-line radio galaxies (Osterbrock, Koski, and Phillips 1976).

At high densities, however, self-absorption (Netzer 1975) and collisional excitation (Kwan and Krolik 1981) also produce substantial deviations from recombination theory. They probably play some role in NGC 7213, since an extrapolation of the optical nonstellar continuum beyond the Lyman limit is grossly inadequate to produce the observed Balmer emission (corrected with $A_v = 2.1$ mag). In particular, the Hα flux expected with the $(\alpha, A_v) = (1.1, 0.61)$ continuum decomposition discussed in § II*b* (and derived in Paper II) and a covering fraction $\lesssim 0.3$ (Paper II) is $\lesssim 3.0 \times 10^{-13}$ ergs s^{-1} cm^{-2}, which is a factor of $\gtrsim 30$ smaller than the dereddened ($A_v = 2.1$) observed flux.

On the other hand, if part of the difference between the observed and theoretical decrements is not caused by dust in the clouds, or if the covering fraction is larger, the calculated shortage of ionizing photons becomes less severe. Moreover, there is no quarantee that the simple extrapolation used above is valid, especially in light of Péquignot's (1984) recent arguments favoring a pronounced maximum in the continuum blueward of the Lyman limit in the Liner NGC 1052. Evidence for a similar feature in NGC 7213 is provided by the possible "UV bump" (Paper II), which may be due to thermal radiation from a hot ($T \sim 8 \times 10^4$ K) accretion disk (Péquignot 1984). Hence, there may in fact be very little discrepancy between theory and observations.

It is interesting to note that NGC 7213 is consistent with Shuder's (1981) strong correlation between the flux of Hα and that of the nonthermal continuum at λ4800 in radio galaxies, type 1 and 2 Seyfert galaxies, and QSOs. This provides good evidence for photoionization, even though the NGC 7213 data, corrected for Galactic extinction ($A_v = 0.05$ mag), show a deficit of nonthermal flux in comparison with the average of Seyfert galaxies. The deficit is within the range observed by Shuder (1981), however, and is reduced substantially if an extinction of 0.61 mag (Paper II) rather than 0.05 mag is

assumed. The "UV bump" discussed above and advocated by Malkan (1983*b*) and Péquignot (1984) can probably account for the remaining discrepancy.

f) *Ultraviolet Emission Lines*

Wu, Boggess, and Gull (1983) noted that the I(C IV λ1550)/I(C III] λ1909) ratio of 1.9 in NGC 7213 is unusually low in comparison with the average of 5 for Seyfert 1 galaxies. The strength of these lines relative to Hβ (Table 1) suggests that they are produced in a region whose ionization parameter (U) is $\sim 10^{-2}$ (Halpern 1982), as expected for the *broad-line* region. It would be important to measure their widths and compare them with the optical forbidden lines to test this hypothesis.

VI. LINERS: PHOTOIONIZATION OR SHOCKS?

Photoionization models involving nonstellar power laws have enjoyed considerable success at explaining the emission lines in Seyfert galaxies and QSOs (e.g., Boksenberg and Netzer 1977; Ferland 1981), especially following the incorporation of improved cross sections for charge-exchange reactions (Butler, Heil, and Dalgarno 1980). In some cases, however, the strong [O III] λ4363 line relative to [O III] $\lambda\lambda$4959 + 5007 is thought to imply temperatures too large to be compatible with photoionized gas. The prototype is NGC 1052, which Fosbury *et al.* (1978) concluded is heated by shocks. Based on their spectral similarity to NGC 1052, Heckman's (1980) Liners are also often regarded as shock heated (Baldwin, Phillips, and Terlevich 1981). On the other hand, the strengths of several lines in the spectrum of NGC 1052 are inconsistent with this (Ferland and Netzer 1983). Moreover, Halpern and Steiner (1983) and Ferland and Netzer (1983) demonstrate that photoionization models having remarkably few free parameters provide adequate agreement with observations if U is low enough. In fact, they see a *continuity* between the characteristics of Seyfert galaxies and Liners which can be reproduced by a systematic variation of U. Liners, for example, show strong emission from neutral and singly ionized species due to relatively low values of U and/or high covering fractions.

This simplicity is a tremendous virtue of the power-law hypothesis. Nevertheless, it has been questioned because of its apparent inability to explain the derived temperatures. But a frequently overlooked fact is that high temperatures result *only* under the assumption that the density in the O^{++} region is comparable to that deduced from the [O II] $\lambda\lambda$3726, 3729 and [S II] $\lambda\lambda$6716, 6731 doublets, which is typically $\sim 10^3$ cm^{-3}. In NGC 7213 this is clearly not the case: n_e is between 10^6 and 10^7 cm^{-3}, and it must be emphasized that the observed [O III] intensity ratio cannot be reproduced at *any* reasonable temperature if $n_e \lesssim 10^{5.5}$ cm^{-3} (Fig. 11). Photoionization models therefore *can* account for the [O III] intensity ratio in NGC 7213, since an excessive T_e is not implied. Moreover, the lines produced by elements in low stages of ionization have a well-understood origin, as their relative intensity ratios do not markedly differ from those in Liners and Seyfert galaxies.

Although shock models can also reproduce many of the observed relative intensities of lines, they do not readily (if at all) explain the presence of [Ne V] λ3426 and broad Balmer emission, and the power-law component visible in the optical spectrum should be absent as well. Moreover, Paper II demonstrates that the X-ray spectrum of NGC 7213 is represented by $f_\nu \propto \nu^{-0.72\pm0.12}$, which is similar to that in many Seyfert galaxies. The compact, flat-spectrum nuclear radio source, "UV bump," and characteristic shape of the continuum from IR through X-ray wavelengths are additional features that have counterparts in other active extragalactic objects (Paper II). Finally, after accounting for the range in gas densities, only He II λ4686 appears considerably weaker than the value predicted by photoionization models, but this is often a puzzle even in classical Seyfert galaxies. A possible solution has been discussed by Péquignot (1984), whose calculations include the effects of a sharp decrease in the number of ionizing photons at energies above $\sim$3–4 ryd.

Thus, there can be little doubt that gas near the nucleus of NGC 7213 is ionized predominantly by nonstellar radiation, although Filippenko (1982*b*) originally conjectured that shocks may be significant. Of course, some shock heating is almost certainly present, given the high observed velocities of clouds, but the effects of the ionizing continuum are probably dominant. The spectrum differs from that of normal Seyfert galaxies due to the lower ionization parameter and wider range of densities in its narrow-line region. In particular, clouds with $n_e \sim 10^6$–10^7 cm^{-3} produce strong [O I] $\lambda\lambda$6300, 6364, [O III] λ4363, and other lines associated with high values of n_e(crit).

An important point to remember is that obvious differences in line width provided the major indication that several distinct regions contribute to the emission-line spectrum in NGC 7213. The analysis was straightforward because lines originating in regions having different densities were not used to derive physical parameters. A number of the Liners discussed by Heckman (1980) show similar behavior (Filippenko 1984; Filippenko and Sargent 1984), so NGC 7213 is not unique. Furthermore, Péquignot (1984) actually uses measured intensity ratios to predict that the gas density in the nucleus of NGC 1052 is stratified in the manner reported here (see § VII). There is no *a priori* reason to suppose, however, that such a clear demarcation of various clouds must occur in every Liner. In particular, regions of high and low n_e *need not* have markedly different velocities. If the narrow-line clouds are moving ballistically away from the nucleus, for example, then the equation of mass continuity implies that $n_e \propto r^{-2}$ (where r is the distance from the nucleus), while the velocity is roughly independent of r. Hence, other galaxies may contain clouds having dissimilar densities whose relative contributions to particular emission lines are not equal, but until now there was no compelling reason for this assumption.

In light of the simplicity of the photoionization hypothesis and its success at explaining the wide range of behavior seen in active galactic nuclei, it would be worthwhile to conduct detailed investigations of many Liners in the manner described here. If the same conclusions can be drawn for a substantial number of cases, then it is possible that a majority of active galaxies are powered by nonstellar radiation produced near a massive central object, as suspected by Keel (1983*a*), Ferland and Netzer (1983), and Halpern and Steiner (1983).

VII. THEORY

a) *General Considerations*

A successful model for the forbidden lines in NGC 7213 must account for the correlation between their width and critical density, FWHM $\propto n_e(\mathrm{crit})^{0.19\pm0.02}$. The following discussion is based on the assumption that photoionization by a nonstellar continuum is the major source of energy input, as argued in § VI. It is also assumed that the FWHM of a line

represents the bulk motion of clouds *whose density is equal to the critical density for that line.* Figure 7 therefore indicates that

$$(v/10^3) = (n/10^6)^{1/5} \quad (2)$$

represents an approximate relation between cloud velocity and density if the units of n and v are cm^{-3} and km s^{-1}, respectively.

Consider clouds in Keplerian orbits, for which $v \propto r^{-1/2}$. One can transform r via $U \propto Ln^{-1}r^{-2}$, where U is the ionization parameter and L is the ionizing luminosity. As long as L is consistent over a dynamical time scale, $v \propto (nU)^{1/4}$. Equation (2) is therefore constant with Keplerian orbits in which U is constant or a very slowly varying function of r. In particular, U must change by less than a factor of 10 while n varies by 10^4.

Approximate constancy of U is an important result of the two-phase model of emission-line regions in QSOs (Krolik, McKee, and Tarter 1981, hereafter KMT), since it reproduces the narrow range actually observed. The broad-line clouds are confined in pressure equilibrium with a hot intercloud medium which is Compton heated by a hard X-ray continuum, and two-phase equilibrium is possible only for a narrow range of U dictated by the atomic physics. This model will be extended to the narrow-line region of NGC 7213, and the existence of a hot confining medium will be demonstrated. Much of what follows parallels discussions in KMT and in Krolik and Vrtilek (1984).

For calculational convenience, the ionizing continuum is represented by a power law with an exponential cutoff at high energies. Specifically,

$$f_\nu = f_0\left(\frac{\nu}{\nu_0}\right)^{-1} \exp\left(\frac{-\nu}{\nu_m}\right) \text{ergs cm}^{-2}\text{ s}^{-1}\text{ Hz}^{-1}\,, \quad (3)$$

where $\nu_0 = 1$ ryd, $\nu_m = 10^4$ ryd, and f_0 is the flux density at the Lyman limit (observed at Earth). U is the dimensionless ratio of ionizing photon density to nucleon density n at the face of a cloud:

$$U = \frac{d^2}{cnr^2}\int_{\nu_0}^{\infty}\frac{f_\nu}{h\nu}\,d\nu \approx \frac{f_0 d^2}{chnr^2}\,, \quad (4)$$

where d is Earth's distance from the object. The dynamical time scale is

$$t_{\rm dyn} = \frac{r}{v} = \frac{d}{v}\left(\frac{f_0}{chnU}\right)^{1/2}. \quad (5)$$

For NGC 7213, $d = 35.4$ Mpc and $f_0 \sim 0.67$ mJy (extrapolating the power law in Fig. 1*b* of Paper II to the Lyman limit), so

$$t_{\rm dyn} \approx 2 \times 10^{11}\left(\frac{10^3}{v}\right)\left(\frac{10^6}{n}\right)^{1/2}\left(\frac{10^{-3}}{U}\right)^{1/2}\text{ s}\,. \quad (6)$$

In the absence of a confining mechanism, a cloud of radius a will expand at roughly the sound speed with time scale $t_{\rm exp} = a/c_s$. Thus,

$$t_{\rm exp} \approx 6 \times 10^9\left(\frac{10^4}{T}\right)^{1/2}\left(\frac{N_{\rm H}}{10^{22}}\right)\left(\frac{10^6}{n}\right)\text{ s}\,, \quad (7)$$

where $N_{\rm H} \sim an$ is the column density. If $T = 10^4$ K and $N_{\rm H} \sim 10^{22}$ cm^{-2} (Kwan and Krolik 1981; Halpern and Steiner 1983), and if $U = 3 \times 10^{-3}$ is typical for Liners (Halpern and Steiner 1983), then $t_{\rm exp}$ is shorter than $t_{\rm dyn}$ for $n \gtrsim 60$ cm^{-3}. Clouds would therefore not survive even one crossing time in the absence of a confining mechanism.

Cold clouds may be confined by a hot intercloud medium (referred to by the subscript h) provided that $n_h T_h$ is large enough. Its minimum density may be derived by assuming that evaporation of the clouds themselves is the only source of gas. Suppose spherical clouds of radius a are uniformly distributed with filling factor F_f (or covering fraction $F_c = 3rF_f/4a$). The equilibrium intercloud density n_h is given by

$$v_h n_h/r = F_f n/t_{\rm exp}\,, \quad (8)$$

where v_h is the velocity with which the intercloud gas leaves the system. Substituting F_c and equation (7) into equation (8), it is found that

$$n_h \approx 2 \times 10^4 F_c\left(\frac{T}{10^4}\right)^{1/2}\left(\frac{n}{10^6}\right)\left(\frac{10^3}{v_h}\right)\text{cm}^{-3}\,. \quad (9)$$

A medium of this density would be sufficient to confine the narrow-line clouds, provided it could be heated to $T_h \gtrsim 10^6$ K. The required heat input to the confining medium can be provided by photoionization, which for $T_h \sim 10^6$ K has the rate $\Gamma_p \sim 10^{-23}$ ergs cm^3 s^{-1} (KMT). The heating time is then

$$t_{\rm heat} = \frac{3kT_h}{n_h\Gamma_p} \approx 4 \times 10^9\left(\frac{T_h}{10^6}\right)\left(\frac{10^4}{n_h}\right)\text{s}\,, \quad (10)$$

which is comparable to $t_{\rm exp}$ but much shorter than the crossing time.

This heating mechanism represents a point of departure from models of the broad-line region. Gas cannot be heated to the Compton equilibrium temperature of $\sim 10^8$ K since the heating time for the Compton process is much longer than the dynamical time scale of the narrow-line region. Instead, the equilibrium T_h may be estimated by balancing the photoionization heating and dynamical times. Combining equations (2), (6), and (10), and invoking pressure equilibrium between the hot medium and cold clouds ($nT = n_h T_h$), yields

$$T_h \approx 7 \times 10^6\left(\frac{n}{10^6}\right)^{3/20}\left(\frac{10^{-3}}{U}\right)^{1/4}\left(\frac{T}{10^4}\right)^{1/2}\text{K}\,. \quad (11)$$

Therefore the temperature range of the hot medium is approximately $2 \times 10^6 \lesssim T_h \lesssim 9 \times 10^6$ K if $10^3 \lesssim n \lesssim 3 \times 10^7$ cm^{-3} and $U = 3 \times 10^{-3}$. Note that "coronal" emission lines of [Fe X] and [Fe XIV] should be negligible since the gas is much more highly ionized than thermal plasma of similar temperature.

The allowed range of ionization parameter in pressure equilibrium is determined by the atomic physics and the spectral shape of the continuum radiation, so it should be comparable for the broad- and narrow-line regions. For QSOs, KMT found $0.3 < \Xi < 10$, where Ξ is proportional to the ratio of radiation pressure to gas pressure and may be somewhat lower in Liners (as suggested by the discussion in § VII*b*). For the spectrum of equation (3),

$$\Xi = \frac{d^2}{cnkTr^2}\int_{\nu_0}^{\nu_1} f_\nu\,d\nu \approx \frac{f_0\nu_0 d^2}{cnkTr^2}\ln\left(\frac{\nu_1}{\nu_0}\right), \quad (12)$$

where $\nu_0 = 1$ ryd and $\nu_1 = 10^3$ ryd. Since the cloud temperature $T \sim 10^4$ K, equations (4) and (12) can be used to obtain

$$U = \left(\frac{kT}{h\nu_0}\right)\frac{\Xi}{\ln(\nu_1/\nu_0)} \approx 0.01\Xi\,. \quad (13)$$

Hence, $3 \times 10^{-3} < U < 10^{-1}$, in reasonable agreement with observations.

The angular size of the emission-line region can be derived from equation (5):

$$\theta = \frac{r}{d} \approx 1.2\left(\frac{10^3}{n}\right)^{1/2}\left(\frac{10^{-3}}{U}\right)^{1/2} \text{ arcsec} . \quad (14)$$

This predicts that the region should be unresolved for $n \gtrsim 10^3$ cm^{-3}.

b) *Comparison with Existing Models*

A constant U, in conjunction with any kinematic model involving Keplerian orbits, produces a $v \propto n^{1/4}$ dependence, and it is encouraging that the observations agree so closely with this "dimensional" argument. Shock models, on the other hand, have difficulty explaining this behavior; they predict no correlation, or at best a continuity, in the velocity of clouds which produce the [O I], [O II], and [O III] lines (among others).

Several detailed models of the narrow-line region have recently been proposed. One of these (Carroll and Kwan 1983, hereafter CK) considers clouds in gravitational infall (parabolic orbits) and explicitly predicts that the line width should increase with n_e(crit). The assumptions of the model include confinement by an isothermal medium and $n \propto r^{-2}$, so that U remains constant with r. In addition, the clouds remain optically thick at all radii so that all ionization stages up to a certain level are present at all velocities. Clouds at $n \sim 10^6$ cm^{-3}, for example, cannot be optically thin to the Lyman continuum, because then [O I] $\lambda\lambda$6300, 6364 could not be produced at high velocities. Outflow models tend to produce optically thin clouds, so in this case line width might correlate better with ionization state than with critical density.

The line widths predicted by CK agree well with the observed velocity widths, except that CK *assume* a relatively strong, narrow component (FWHM $\sim$ 250 km s^{-1}) in each line, which is supposed to arise in a reservoir of low-density gas. The net effect is to drastically reduce the variation of FWHM relative to that of FWZI. No significant differences between FWHM and FWZI are observed in Figure 7, which argues against a large reservoir of low-density gas in NGC 7213. The line intensity *ratios* predicted by the model are also not in good agreement with observations of NGC 7213, since parameters of the model were obviously adjusted to best fit the "average" Seyfert galaxy, whose ionization level is higher than that of Liners. Note, however, that the predicted ratio I([O III] λ5007)/I([O III] λ4363) = 5 for the infalling clouds alone (neglecting the narrow-line reservoir) agrees perfectly with the observations (Table 1).

CK successfully explain the blueshifted centroids of forbidden lines, which are especially prominent among [Ne V], [Ne III], and [O III]. Although the clouds are in Keplerian orbits, emission during outflow is much weaker than that from the inward leg. If the clouds contain appreciable quantities of dust, then infalling clouds on the far side of the continuum source will be preferentially seen, resulting in a net blueward asymmetry. As discussed in § V*d*, this asymmetry need not be present in all of the lines. It is also entirely consistent with a constant value of U, particularly since various lines are emitted by different clouds. Furthermore, U can vary by up to a factor of ten in NGC 7213 (§ VII*a*), thereby producing additional stratification in the line-emitting zones.

The CK model applies only if gravity dominates over radiation pressure, and hints that a property which distinguishes NGC 7213 and other Liners from "normal" Seyfert galaxies may be an abnormally low ratio of ionizing flux to central mass. For an optically thick cloud it is necessary that

$$M > L_{\rm ion}/(4\pi c G m_{\rm H} N_{\rm H}) \text{ g} , \quad (15)$$

where $m_{\rm H}$ is the mass of a hydrogen atom and $L_{\rm ion}$ is the luminosity between 1 and $\sim$100 ryd. Thus,

$$\left(\frac{M}{M_\odot}\right) > 1.2 \times 10^7 \left(\frac{10^{22}}{N_{\rm H}}\right)\left(\frac{L_{\rm ion}}{10^{43}}\right) , \quad (16)$$

and $M \sim 2 \times 10^7\ M_\odot$ would be sufficient for gravity to dominate in NGC 7213 ($L_{\rm ion} \sim 1.5 \times 10^{43}$ ergs s^{-1}). The mass derived assuming Keplerian orbits and $U = 3 \times 10^{-3}$ is $\sim 4 \times 10^8\ M_\odot$, consistent with equation (16). This simple argument neglects other forces, such as drag by the hot intercloud medium.

Krolik and Vrtilek (1984, hereafter KV) discuss a dynamical model which consists of an outflowing hot wind in a logarithmic potential. The clouds are assumed to be entrained in the wind, and line profiles are generated for both adiabatic and nonadiabatic flows. Although KV do not explicitly consider the effects of n_e(crit) in calculating line profiles, some restrictions can be placed on the parameters of their model. Only the adiabatic solutions agree with the observations in that they decelerate with increasing r, and a consequence of this is that the temperature of the hot medium cannot increase with radius. In addition, the flow is likely to be supersonic everywhere since the sound speed in a gas having $T_h = 10^6$ K is only $\sim$100 km s^{-1}. The adiabatic, supersonic solutions have the property that U is nearly independent of r, whereas v decreases slowly. These are exactly the conditions which are inferred from the observed line widths, so that the KV model could in principle be made consistent with the data. Since KV display only one supersonic model, adjustments in additional parameters will be necessary in order to test for quantitative agreement. It also remains to be seen if the outflowing clouds can stay optically thick over a sufficient range in radius to maintain species having low ionization at both low and high velocity.

A similar model is considered by Carleton (1984). Gas which produces the broad lines flows radially into the narrow-line regions (or vice versa), and the emission of the gas is integrated over its lifetime. Carleton (1984) correctly predicts that the widths of forbidden lines should increase with n_e(crit), and the calculated profiles of emission lines resemble those in NGC 7213 (especially in the case of [O I] $\lambda\lambda$6300, 6364). These predictions are also made by Péquignot (1984), and the density stratification on which his models are based is strongly supported by the observations of NGC 7213.

To conclude, it appears that simple kinematic arguments can account for the general behavior of velocity width versus critical density. Detailed fitting of the line strengths and profiles may in the future discriminate between the various dynamical models which have been proposed. At present, the model by CK seems to most naturally explain the data in a quantitative manner.

VIII. SUMMARY

New optical spectra of the nearby S0 galaxy NGC 7213 are analyzed. Because of the presence of a very strong stellar component, a major effort is made to accurately subtract the optical spectrum of an appropriate template galaxy, yielding

the uncontaminated emission-line spectrum. Failure to properly remove the absorption lines in previous studies of similar galaxies is probably responsible for overestimates of the strength of weak lines such as [O III] λ4363, which is situated at a high point in the normal stellar continuum.

The following conclusions are drawn in this study:

1. Many of the main characteristics of type 1 Seyfert galaxies are exhibited by the nucleus of NGC 7213. These include broad Balmer emission and forbidden lines of highly ionized species. In addition, Paper II reports the presence of a power-law X-ray spectrum, significant nonstellar flux at optical wavelengths, and possibly a "UV bump." By analogy with classical active extragalactic objects, photoionization is clearly the gas excitation mechanism. On the other hand, the great strength of [O III] λ4363 relative to [O III] $\lambda\lambda$4959 + 5007 is reminiscent of the high temperatures seen in shock-heated gas, and initially seems inconsistent with photoionization by a nonstellar continuum. Furthermore, prominent emission from neutral and singly ionized species (e.g., [O I] λ6300) suggests that the gas may be heated by shocks, as has been proposed for Liners.

2. The observations are reconciled with photoionization models by the discovery that densities of order 10^6–10^7 cm^{-3} exist in the narrow-line region. At such high densities, auroral [O III] λ4363 emission is greatly enhanced even at the usual temperature of photoionized gas ($\sim 10^4$ K). Moreover, strong lines from many species of low ionization are produced if the ionization parameter is small and the density is high.

3. Low-density clouds are also present in the emission-line region, as shown by the relative intensities of the nebular [O II] and [S II] doublets. These lines are much narrower than the auroral and transauroral components of the *same species*, whose widths are comparable to those of [O III]. This implies that clouds having *very different bulk motions and densities* exist near the nucleus of NGC 7213. Such diversity in the narrow-line region is unprecedented in the study of active galactic nuclei.

4. There is a strong correlation between the width of an emission line and the critical density of the upper level from which the corresponding electron transition occurs. Since any line is most efficiently produced at densities near or just above the critical value if a sufficiently large range of densities is present, this supports the conclusion in (3).

5. The observed relationship between velocity width and density ($v \propto n^{1/5}$) is consistent with clouds moving in Keplerian orbits while maintaining a nearly constant ionization parameter. This can be understood by a natural extension of the two-phase model of QSO emission-line regions. Strong density stratification is a feature of several other theoretical studies as well.

6. The Balmer decrement indicates $A_v = 2.1$ mag in the absence of other effects. A simple extrapolation of the nonstellar continuum (derived in Paper II) to UV wavelengths is inadequate by roughly a factor of 10 to produce the dereddened Balmer intensities even if the covering fraction is unity, so collisional excitation and radiative transfer probably alter the Case B decrement. Additional ionizing photons from the "UV bump" might alleviate any remaining discrepancy.

7. This investigation may contain a key to the nature of Liners, whose spectra have been well explained by photoionization models *except* for the high temperature ($T_e \gtrsim 25000$ K) sometimes derived from the nebular to auroral [O III] intensity ratio. Due to this discrepancy, and to the strong lines from neutral and singly ionized species, emission in Liners has often been attributed to heating by shocks. On the other hand, if high densities and large ranges in density are present, as in the case of NGC 7213, the temperature of the ionized gas need not be high to explain the relative line intensities. Photoionization by a nonstellar continuum is then the most likely mechanism of gas excitation, and the low-ionization lines indicate that the ionization parameter is lower than in classical Seyfert galaxies.

It is a pleasure to thank S. A. Shectman, G. Yanik, and K. Clardy for the design, construction, and maintenance of the hardware and software associated with the Intensified Reticon detector at Las Campanas Observatory. The enthusiastic help of night assistants A. Guerra and F. Peralta, and of day assistants H. Solis and W. Robinson, is greatly appreciated. Useful discussions were enjoyed with W. L. W. Sargent, J. B. Oke, M. Elvis, N. P. Carleton, D. P. Schneider, M. A. Malkan, and W. C. Keel. An anonymous referee made many valuable remarks. Thanks are due to P. J. Young for the data reduction program (LOLITA) and to T. J. Pearson for much of the software used to produce the figures. Some of the results in this paper were presented by A. V. F. at a workshop on "Ionization Mechanisms in Emission-Line Nuclei of Galaxies" (Pagel and Edmunds 1983). The Fannie and John Hertz Foundation provided financial assistance to A. V. F. through a graduate fellowship, and additional support was obtained from NSF grant AST 82-16544 to W. L. W. Sargent and NASA grant NGL 05-002-134 to J. B. Oke. Observations were made as part of the cooperative agreement between the Carnegie Institution of Washington and Caltech.

REFERENCES

Baldwin, J. A. 1975, *Ap. J.*, **201**, 26.
Baldwin, J. A., Phillips, M. M., and Terlevich, R. 1981, *Pub. A.S.P.*, **93**, 5.
Baluja, K. L., Burke, P. G., and Kingston, A. E. 1981, *J. Phys. B*, **14**, 119.
Boksenberg, A., and Netzer, H. 1977, *Ap. J.*, **212**, 37.
Bowen, I. S. 1960, *Ap. J.*, **132**, 1.
Brocklehurst, M. 1971, *M.N.R.A.S.*, **153**, 471.
Burgess, A. 1958, *M.N.R.A.S.*, **118**, 477.
Burstein, D., and Heiles, C. 1982, *A.J.*, **87**, 1165.
Butler, S. E., Heil, T. G., and Dalgarno, A. 1980, *Ap. J.*, **241**, 442.
Carleton, N. P. 1984, preprint.
Carroll, T. J., and Kwan, J. 1983, *Ap. J.*, **274**, 113 (CK).
Dalgarno, A., and Sternberg, A. 1982, *Ap. J. (Letters)*, **257**, L87.
Danziger, I. J., Fosbury, R. A. E., and Penston, M. V. 1977, *M.N.R.A.S.*, **179**, 41P.
Dopita, M. A. 1977, *Ap. J. Suppl.*, **33**, 437.
Ferland, G. J. 1981, *Ap. J.*, **249**, 17.
Ferland, G. J., and Netzer, H. 1983, *Ap. J.*, **264**, 105.
Filippenko, A. V. 1982*a*, *Pub. A.S.P.*, **94**, 715.
———. 1982*b*, *Bull. AAS*, **14**, 947.
———. 1984, *Ap. J.*, submitted.
Filippenko, A. V., and Greenstein, J. L. 1984, *Pub. A.S.P.*, **96**, in press.
Filippenko, A. V., and Sargent, W. L. W. 1984, *Ap. J. Suppl.*, submitted.
Fosbury, R. A. E., Mebold, U., Goss, W. M, and Dopita, M. A. 1978, *M.N.R.A.S.*, **183**, 549.
Garstang, R. H. 1968, in *IAU Symposium 34, Planetary Nebulae*, ed. D. E. Osterbrock and C. R. O'Dell (Dordrecht: Reidel), p. 138.
Giles, K. 1979, *M.N.R.A.S.*, **187**, 49P.
Halpern, J. P. 1982, Ph.D. thesis, Harvard University.
Halpern, J. P., and Filippenko, A. V. 1984, *Ap. J.*, **285**, 475 (Paper II).
Halpern, J. P., and Steiner, J. E. 1983, *Ap. J. (Letters)*, **269**, L37.
Heckman, T. M. 1980, *Astr. Ap.*, **87**, 152.
Heckman, T. M., and Balick, B. 1979, *Astr. Ap.*, **79**, 350.
Heiles, C., and Cleary, M. N. 1979, *Australian J. Phys. Ap. Suppl.*, No. 47, p. 1.
Kafatos, M., and Lynch, J. P. 1980, *Ap. J. Suppl.*, **42**, 611.
Keel, W. C. 1983*a*, *Ap. J.*, **269**, 466.
———. 1983*b*, *Ap. J. Suppl.*, **52**, 229.
Keel, W. C., and Miller, J. S. 1983, *Ap. J. (Letters)*, **266**, L89.
Koski, A. T. 1978, *Ap. J.*, **223**, 56.
Koski, A. T., and Osterbrock, D. E. 1976, *Ap. J. (Letters)*, **203**, L49.
Krolik, J. H., McKee, C. F., and Tarter, C. B. 1981, *Ap. J.*, **249**, 422 (KMT).

Krolik, J. H., and Vrtilek, J. 1984, *Ap. J.*, **279**, 521 (KV).
Kwan, J., and Krolik, J. H. 1981, *Ap. J.*, **250**, 478.
Lequeux, J., Peimbert, M., Rayo, J. F., Serrano, A., and Torres-Peimbert, S. 1979, *Astr. Ap.*, **80**, 155.
Malkan, M. A. 1983*a*, *Ap. J.* (*Letters*), **264**, L1.
———. 1983*b*, *Ap. J.*, **268**, 582.
Mendoza, C., and Zeippen, C. J. 1982, *M.N.R.A.S.*, **198**, 127.
Netzer, H. 1975, *M.N.R.A.S.*, **171**, 395.
Nussbaumer, H., and Rusca, C. 1979, *Astr. Ap.*, **72**, 129.
Nussbaumer, H., and Storey, P. J. 1981, *Astr. Ap.*, **99**, 177.
Oke, J. B., and Gunn, J. E. 1983, *Ap. J.*, **266**, 713.
Osterbrock, D. E. 1974, *Astrophysics of Gaseous Nebulae.* (San Francisco: Freeman).
———. 1981, *Ap. J.*, **246**, 696.
Osterbrock, D. E., Koski, A. T., and Phillips, M. M. 1976, *Ap. J.*, **206**, 898.
Pagel, B. E. J., and Edmunds, M. G. 1983, *Nature*, **304**, 488.
Pelat, D., and Alloin, D. 1980, *Astr. Ap.*, **81**, 172.
———. 1982, *Astr. Ap.*, **105**, 335.
Pelat, D., Alloin, D., and Fosbury, R. A. E. 1981, *M.N.R.A.S.*, **195**, 787.
Péquignot, D. 1984, *Astr. Ap.*, **131**, 159.
Péquignot, D., and Aldrovandi, S. M. V. 1976, *Astr. Ap.*, **50**, 141.
Phillips, M. M. 1978, *Ap. J. Suppl.*, **38**, 187.
———. 1979, *Ap. J.* (*Letters*), **227**, L121.
Pradhan, A. K. 1974, *J. Phys. B*, **7**, L503.
———. 1976, *M.N.R.A.S.*, **177**, 31.
———. 1978, *M.N.R.A.S.*, **183**, 89P.
Rose, J. A., and Tripicco, M. J. 1984, *Ap. J.*, **285**, 55.
Sadler, E. M. 1984, *A.J.*, **89**, 23.
Sandage, A. R., and Tammann, G. A. 1981, *A Revised Shapley-Ames Catalog of Bright Galaxies* (Washington: Carnegie Institution of Washington).
Schneider, D. P., and Young, P. 1980, *Ap. J.*, **238**, 946.
Seaton, M. J. 1975, *M.N.R.A.S.*, **170**, 475.
Shectman, S. A., and Hiltner, W. A. 1976, *Pub. A.S.P.*, **88**, 960.
Shuder, J. M. 1981, *Ap. J.*, **244**, 12.
———. 1982, *Ap. J.*, **259**, 48.
Shull, J. M., and McKee, C. F. 1979, *Ap. J.*, **227**, 131.
Stauffer, J. R. 1982, *Ap. J.*, **262**, 66.
Whitford, A. E. 1958, *A.J.*, **63**, 201.
Wu, C.-C., Boggess, A., and Gull, T. R. 1983, *Ap. J.*, **266**, 28.
Yee, H. K. C., and Oke, J. B. 1978, *Ap. J.*, **226**, 753.
Zeippen, C. J. 1982, *M.N.R.A.S.*, **198**, 111.

Note added in proof.—Private communications indicate that some confusion exists concerning the exact definition of a "Linear," the classification of NGC 7213, and the relationship between these objects; hence, a few brief remarks are necessary. Heckman (1980) arbitrarily defined Liners to be galactic nuclei in which "[O II] λ3727 is at least as strong as [O III] λ5007 and in which [O I] λ6300 is at least one-third as strong as [O III] λ5007." Galaxies near this dividing line were called "transition" objects. Notice that the above definition contains *no* reference to the presence or absence of a nonstellar continuum or broad permitted emission lines. Thus, although NGC 7213 is clearly a Seyfert 1 galaxy in many respects (e.g., broad Hα, X-rays, nonstellar continuum, [Ne V] λ3426), it is *also* almost a Liner because I([O II] λ3727)/I([O III] λ5007) $\sim$ 0.43 and I([O I] λ6300)/I([O III] λ5007) $\sim$ 0.83 (see Table 1). As is shock-heated gas, forbidden lines of low ionization (and [O III] λ4363) are abnormally intense compared with those in typical Seyferts. The transition galaxy NGC 7213 therefore provides an excellent opportunity to gain an understanding of "shock" features in the context of *photoionization* models, and this is precisely why it may be a key to the nature of "classical" Liners which satisfy *both* of Heckman's (1980) criteria.

ALEXEI V. FILIPPENKO: Department of Astronomy, University of California, Berkeley, CA 94720

J. P. HALPERN: Department of Physics, Columbia University, 538 West 120th Street, New York 10027